Global Patterns Predict Local Biodiversity Shifts in a Climate Change Hotspot

Jake A. Lawlor[1], Amelia V. Hesketh[2], Julien Beaulieu[3,4], Nicole S. Knight[5], Tianna Peller[6], Laura Super[5], Alexis Pereira[7], Ellen K. Bledsoe[8], Joseph B. Burant[9], Jennifer A. Dijkstra[10], Kylla Benes[11,12], Jarrett E.K. Byrnes[13]

1. Department of Biology, McGill University
2. Simon Fraser University, School of Resource & Environmental Management
3. Département des Sciences Biologiques, Université du Québec à Montréal
4. Groupe de Recherche Interuniversitaire en Limnologie (GRIL)
5. University of British Columbia
6. University of Toronto, Department of Ecology and Evolutionary Biology
7. University of Guelph
8. School of Natural Resources and the Environment, University of Arizona
9. Department of Animal Ecology, Netherlands Institute of Ecology
10. School of Marine Science and Ocean Engineering, Center for Coastal and Ocean Mapping
11. Davidson Honors College, University of Montana
12. Shoals Marine Lab, University of New Hampshire
13. Department of Biology, University of Massachusetts Boston

Corresponding Author: Jake Lawlor; jake.lawlor@mail.mcgill.ca

Abstract

Climate change is redistributing life on Earth, and global-scale biogeographical patterns can inform expectations for local ecological responses. As thermal envelopes shift towards higher absolute latitudes and deeper depths in the ocean, fixed locations are experiencing changes in their niche space, driving changes in abundance, occurrence, and community composition. Here, we examine intertidal population and community change in a climate-warming hotspot using a dataset of intertidal surveys collected over a 42-year duration on Appledore Island in the Gulf of Maine, USA, paired with global occupancy-derived estimates of species' thermal niches. We quantify changes that have occurred and test whether observed changes align with expectations informed by global-scale trends. We detect several signals consistent with climate-driven biodiversity change: appearance and increased abundance of warm-affinity species, disappearance and decreased abundance of cold-affinity species, overall increases in species richness, shifts of species richness towards lower tidal elevations, and increases in community temperature affinity, which notably lags the rate of temperature change by a factor of six. In contrast, we find little evidence for shifts in individual species' distributions across intertidal elevations, suggesting that community change overall and across intertidal elevations might be driven more strongly by within-range abundance shifts than by wholesale redistributions. These findings exemplify that community-level metrics can be more sensitive indicators of climate-driven change than species-level distribution shifts, particularly given limits on data resolution. Overall, our results provide strong evidence of climate-driven reorganization in Appledore Island's intertidal community and demonstrate how long-term datasets from static locations can be contextualized with global-scale data to infer broad biological responses to climate change.

Keywords:

Climate Change Ecology, Marine Ecology, Range Shifts, Intertidal Ecology, Biogeography, Thermal Tolerance

Introduction

Climate change is shifting the distribution of life on Earth, with warming temperatures driving species generally towards higher latitudes, higher elevations, and deeper depths in the ocean (Lawlor et al., 2024; Lenoir et al., 2020; Pecl et al., 2017). These distribution shifts are thought to be related to species' thermal tolerances (Sunday et al., 2012) and are particularly evident in ectothermic, high-latitude, and marine species (Lenoir et al., 2020; Ramalho et al., 2023). As temperatures warm and thermal envelopes shift across space, species' geographic ranges can contract at warm range edges when temperatures surpass thermal maxima or expand at cool edges when temperatures exceed thermal minima, although a variety of biological and environmental factors influence the extent to which ranges can or will shift (Billman et al., 2025; Krumhansl et al., 2024; Lawlor et al., 2024; Sunday et al., 2012, 2015). Even within species' geographic ranges, sublethal changes in temperature can shift species' abundances as warming causes populations to experience conditions that are closer to or further from their thermal optima (Rubenstein et al., 2023). Populations in the colder-than-optimum portion of a species' range might therefore experience positive changes in performance and fitness as temperatures increase, translating to increases in abundance. In contrast, populations at the warmer-than-optimum portion of a species' range can experience negative changes in performance and fitness as temperatures warm, leading to decreases in abundance and potentially extirpation (Hastings et al., 2020; Lenoir & Svenning, 2013).

Shifts in individual species' ranges can drive changes in community structure and composition (Antão et al., 2022; Siwertsson et al., 2024; Telwala et al., 2013), and such changes are already observable in marine ecosystems at macroecological scales. Across global oceans, peaks of species richness have shifted away from the equator since the 1950s, shifting the Latitudinal Biodiversity Gradient for marine species from a single peak at the equator to a bimodal distribution peaking around 20° North and South (Chaudhary et al., 2021). Deep-time patterns suggest that these shifting biodiversity peaks might reflect distributions of life similar to those in previous hot-house Earth periods, when richness was typically highest at temperate rather than tropical latitudes (Mannion et al., 2014). Within species' ranges, abundances have also changed, with population increases typically observed in poleward portions and decreases usually seen in equatorward portions (Hastings et al., 2020). As a result, marine communities have undergone thermophilization (Vergés et al., 2019; Zarzyczny et al., 2023), marked by the decline or loss of cold-affinity species, the proliferation or introduction of warm-affinity species, or the increase in

temperature affiliation of the community (Community Temperature Index; CTI) (Barry et al., 1995; Burrows et al., 2020; Day et al., 2018). Although warming-driven changes to marine ecosystems have been repeatedly observed (Mieszkowska, 2025), the extent to which changes can be generalized or predicted is unclear. In order to fill this gap, we need high-resolution temporal observations of biodiversity change in warming marine environments, which can reveal factors underlying biodiversity change and the effects of species-level changes on communities and ecosystems.

Intertidal habitats present an ideal model system to study the effects of warming on biodiversity. Similar to montane environments on land, intertidal environments generally exist along two thermal gradients: (1) a large-scale thermal gradient across latitudes and (2) a small-scale thermal gradient from high to low intertidal elevations, although nonlinearities owing to factors like tidal regimes and shore features (e.g., slope, aspect, and topography) can exist (Helmuth et al., 2002, 2006; Helmuth & Hofmann, 2001). Intertidal species are therefore subject to limitations—both temperature-related and otherwise—at maximum and minimum latitudes of occurrence, as well as at upper and lower elevational limits within the intertidal zone, offering multiple points of assessment for responses to climate change. Generally, latitudinal distributions of intertidal species are set by interactions of water temperatures, air temperatures, and tidal fluctuations, which form thermal and desiccation stress gradients across space (Helmuth et al., 2006) and can be further bound by biogeographic breaks or circulation patterns that prevent propagules from reaching otherwise-suitable regions (García Molinos et al., 2017; Krumhansl et al., 2023). Elevational limits have slightly different drivers: upper limits of intertidal distributions are thought to be set by thermal and desiccation tolerance during emersion at low tide, with thermal stress tending to decrease at lower tidal elevations (Blouin et al., 2011; Connell, 1972; Drake et al., 2017; Harley & Helmuth, 2003). Alternatively, lower limits are more strongly set by biotic factors like competition and predation pressure (Connell, 1961, 1972; Harley & Helmuth, 2003; Wethey, 1983). Changes in intertidal thermal environments could therefore directly affect distribution limits at high latitude, low latitude, and high elevation edges, with low elevation edges more likely to remain stable, at least as a result of the direct pressures of temperature change.

In addition to the multidimensional thermal landscape, intertidal ecosystems largely comprise species that are ectothermic and have limited or no adult mobility; since individuals are unable to track moving temperature envelopes across large distances, responses to warming should be observable in the growth or survival of populations. Expected effects of warming in intertidal

environments include the arrival, increase, decrease, or extirpation of species as their latitudinal thermal envelopes shift across study locations, but could also vary across intertidal elevations, with species shifting lower on shore to avoid increasing thermal stress in the upper intertidal zone. Some studies have documented latitudinal shifts in intertidal species (Fenberg & Rivadeneira, 2011; Jones et al., 2012; Mieszkowska, 2016; Sunday et al., 2015), thermophilization of intertidal communities (Barry et al., 1995; Burrows et al., 2020), thermally-linked abundance changes (Mieszkowska et al., 2021; Sato et al., 2025), or shifts in vertical distributions of species (Harley, 2011; Harley & Paine, 2009) in response to warming climates, but few have assessed both species- and community-level responses in the context of latitudinal and elevation gradients over long timeframes simultaneously.

While global-scale bodies of work suggest coherent biogeographic responses to climate change (Lawlor et al., 2024; Lenoir et al., 2020; Parmesan & Yohe, 2003), tracking shifts in individual species or higher-order biodiversity variables (e.g., richness) remains difficult. The most detailed documentations of biodiversity shifts come from high-resolution species occurrence data collected over large spatial and temporal scales, but data of these quantities are not available for most species or in most locations, thus biasing global bodies of work towards data-rich species and locations. However, due to the increased availability of species occurrences from databases such as the Global Biodiversity Information Facility (GBIF) and the Ocean Biodiversity Information System (OBIS), and international efforts to produce long-term reconstructions of environmental variables, it is now possible to contextualize species-specific changes occurring in single locations over time with their broader historical niche spaces (Webb et al., 2020). These derived environmental niches can be used to explain and predict species occurrence or abundance patterns (Sato et al., 2025), thus testing support for global patterns in static locations over time (Givan et al., 2018; Mieszkowska et al., 2021). Given that marine invertebrates and algae together make up only 2.5% of species latitudinal and elevational shift documentations, and “intertidal habitats” and “rocky shores” make up only 5% of documented tropicalization events in two recent syntheses (Comte et al., 2020; Zarzyczny et al., 2023), proximal indicators of consistency with global trends could help to demystify the biological responses of intertidal taxa and ecosystems to climate change.

Here, we assess long-term changes in intertidal community composition in the Gulf of Maine, a region that warmed faster than 99% of global oceans during the 2000s (Pershing et al., 2015) and in which warming-associated community change in the intertidal zone remains unassessed

(Zarzyczny et al., 2023). We use 40 years of intertidal species presence and abundance data collected along permanent transects on Appledore Island in Maine, USA, paired with thermal affinity estimates derived from global species occurrence data to assess species- and community-level patterns of change. Given that climate warming is occurring rapidly in this region (Fig. S1), we use global-scale patterns of biodiversity responses to inform seven hypotheses—three species-specific and four at the community level—of climate responses in the Appledore Island intertidal community, both as a whole and across intertidal heights (Fig. 1):

Species-Specific Hypotheses:

1. If temperature drives species establishment and extirpation across latitudes, warm-affinity species should appear and cold-affinity species should disappear from the Appledore Island community over time.
2. If temperature drives vertical zonation patterns in the intertidal zone, species should shift towards lower intertidal elevations over time, particularly at their upper distributional limits.
3. If temperature drives species' abundance, warm-affinity species should increase in abundance and cool-affinity species should decrease in abundance over time.

Community-Level Hypotheses:

4. If warming is shifting global biodiversity peaks from the equator towards temperate regions, overall species richness should increase on Appledore Island over time.
5. If warming shifts species' vertical distributions towards lower elevations, richness should decrease in the upper intertidal zone and increase in the lower intertidal zone.
6. If temperature drives community assemblages, the overall community temperature index should increase over time.
7. If warming causes higher-elevation species to shift down shore, community temperature index should increase across intertidal levels.

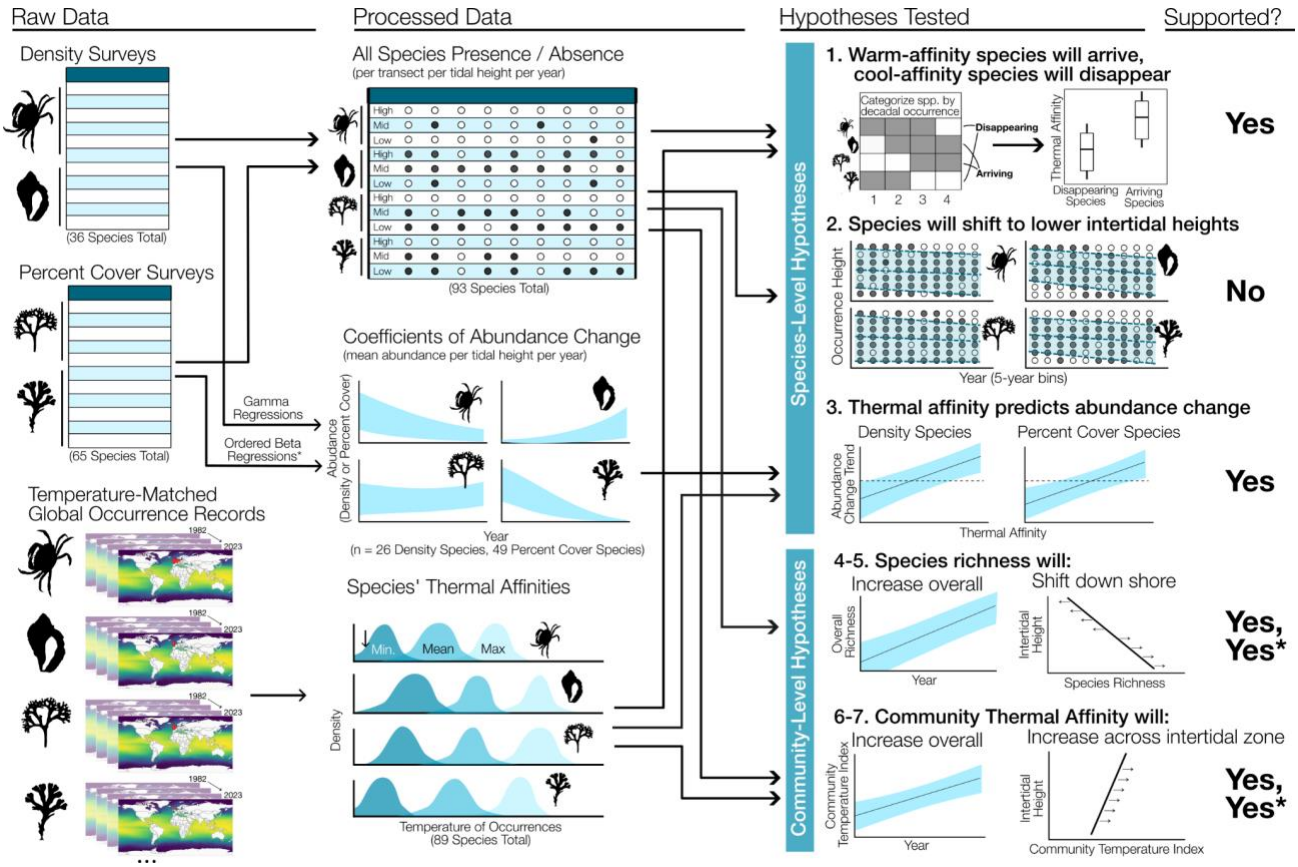

Figure 1. Conceptual diagram of data, processing pipelines, hypotheses, and results for assessments of climate responses in the Appledore Island intertidal community. The leftmost column shows input data, including density and percent cover surveys from Appledore Island over 40 years of sampling and global occurrences of each species from Ocean Biodiversity Information System (OBIS). The second column shows derived data, including species' presences and across intertidal heights over time, coefficients from abundance change models, and occupancy-derived thermal affinities. The third column lists hypotheses tested, which are informed by global trends, and the rightmost column indicates whether or not hypotheses were supported from our data and analyses; asterisk indicates support for our hypothesis but with a slightly different relationship than we expected.

Methods

Intertidal Data

To assess changes in intertidal biodiversity in this climate warming hotspot, we used a long-term dataset of surveys on Appledore Island in Maine, USA, collected during summer from 1982 to 2023 (excluding 2007 and 2018) by undergraduate students at the Shoals Marine Laboratory (Shoals Marine Laboratory, 2018). The dataset includes marine invertebrate and macroalgae community surveys along 21 permanent vertical transects distributed around the perimeter of Appledore Island, denoted by permanent markers in the bedrock at 4.11m above chart datum.

During each visit, replicate quadrats (n = 1–4) were sampled at 0.33 m (1 ft) intervals along transects, from the highest interval at which organisms were observed to the lowest accessible interval (as constrained by tides, wave conditions, etc.). Sampled quadrats ranged from 5.33 m above chart datum to -1.68 m below chart datum. Within each quadrat, all organisms were identified to the lowest possible taxonomic denominator, and observations of organisms at the species level were retained. Usually, abundance data were recorded, either as (1) counts per quadrat—extrapolated to densities per m^2—for non-colonial invertebrate species (e.g., snails, urchins, sea stars), and (2) percent cover for colonial or bed-forming invertebrates (e.g., barnacles, mussels) and macroalgal species (canopy cover). The number of transects, shore levels, and replicate quadrats varied from year to year, but included observations of 93 total species, with up to 50 species recorded within a single year of sampling. Because some of the response variables tested in our models (e.g., richness, distributional limits) are likely to be affected by sampling effort and irregularities, we additionally produced a subset of the full dataset, limited to only transects, intertidal heights, and years that were consistently sampled throughout the study period (totaling seven transects across nine intertidal heights in 37 years of sampling, see Fig. S2 for details), which we hereafter refer to as the *highly sampled dataset*. We used the highly sampled dataset in analyses for which differences in sample size or domain were likely to affect the response variable, but used the full dataset in other analyses where maximizing data retention was more appropriate.

Thermal Affinities

We calculated occupancy-derived thermal affinities using methods adapted from Webb (2020), which have consistently and robustly correlated with experimentally-derived thermal tolerance limits of marine species despite variations in record resolution and bias (Webb et al., 2020). We collected occurrence records from OBIS (OBIS, 2025) for all species detected in the intertidal survey dataset, filtering to occurrence records from coastal regions shallower than 10m depth and dating from 1982–2023. We matched occurrence records to temperature values from the Hadley Centre Sea Ice and Sea Surface Temperature (HadISST) 1° resolution monthly Global Sea Surface Temperature dataset within the year and grid cell of occurrences, producing temperature-matched occurrence records for 89 of 93 species, ranging from 8 to 57,328 temperature-matched occurrences per species (median = 1,978). For each occurrence record, we collected the warmest and coldest monthly mean temperature from the year of each observation, and the mean of monthly mean temperatures (hereafter, *annual mean*). We calculated three proximal indices of

species' thermal affinities: (1) thermal minima, the 5th percentile of coldest-month temperatures of global occurrences, (2) mean thermal affinity, the mean of all annual mean temperatures of global occurrences, and (3) thermal maxima, the 95th percentile of hottest-month temperatures of global occurrences (Fig. S3). Following Webb (2020), we primarily use the mean thermal affinity for thermal-affinity-based analyses, but use minimum and maximum values for some additional tests.

Species Distribution Shifts

Although occurrence data collected solely on Appledore Island cannot facilitate direct measurements of species' range shifts across latitudes, we used species' appearances and disappearances in the Appledore Island community over time as indicators of occurrence change within this cross-section of species' latitudinal ranges. In order to sort species by their occurrence patterns over time, we summarized observations from the highly sampled dataset into four temporal bins (two ten-year and two eleven-year bins of the 42-year sampling span) and categorized species into four groups: (1) disappearing species, present in the time first bin and absent in the last; (2) arriving species, present in the last time bin but not in the first; (3) persistent species, present in all bins; and (4) rare/other species, species that did not fit into the previous categories (Fig. 2a,b). We then tested for differences in thermal affinities (mean, minimum, and maximum) among species in the four groups using one-way ANOVAs and pairwise Tukey comparisons (Fig. 2c–e). Because species arriving to the community could either represent range-shifting species from neighboring regions or introduction of non-native species, we categorized every species by its origin into "native" and "non-native" and tallied proportions of each within each occurrence-based group (Fig. 2a,b).

To assess changes in vertical distributions of individual species within the intertidal zone, we analyzed species occurrences (presence/absence) within the highly sampled dataset, combining occurrences from both datasets (density and percent cover surveys). For each species in each year, we calculated the minimum (5th percentile), median, mean, and maximum (95th percentile) intertidal height at which the species was present across all transects and replicate quadrats, then used linear regressions to model each of the four parameters as a function of sample year (Fig. S4). We included only species present in 10 or more years of survey data, totaling assessments of vertical distribution shifts for 43 species. We extracted the slopes of all regression models to find the direction of change (upwards or downwards) of each distributional range parameter, as

well as the *p*-value of the fit to assess significance. Because species with distribution ranges bordering the edge of the sampling domain might not show detectable shifts (e.g., if an edge shifts outside of the sampling domain), we conducted a sensitivity test that excluded: upper edge shifts when over 50% of a species' maximum yearly occurrences were at the highest sampled height; lower edge shifts when over 50% of a species' minimum yearly occurrences were at the lowest sampled height; and mean and median shifts when both previous cases were met (Fig. S4, S5). In addition to the combined dataset, we repeated this process using occurrences from only the density and only the percent cover datasets, respectively.

Abundance Changes

Recording abundances as both density and percent cover resulted in data with two different distributions (0–infinity for density; 0–100 for percent cover); thus, we analyzed abundance change trends separately for these two groups of species. Abundance values (density and percent cover) were measured within 1–4 replicate quadrats spanning up to 21 intertidal heights within 21 transects (Fig. S2), but sampling resolution varied widely through time, presenting complications when accounting for these factors in models. For example, some shore levels were only sampled in one or few years of the time series, while others were sampled in all 40, and some transects stopped being sampled as protocols changed across the 40 surveyed years (Fig. S2). Additionally, some species were present only a few times throughout the time series but within different transects, preventing models from converging if transect ID was included as a random factor. For these reasons, we condensed the response variable of both models to the average annual abundance (density or percent cover) within each intertidal height, summarized across all transects. To arrive at this summarized response variable, we averaged abundance within 1–4 replicates of each quadrat (mean = 2.4), then averaged all quadrat values within each tidal elevation for every year (1–17 quadrats, mean = 5.9 for density species; mean = 5.1 for percent cover species). We additionally filtered to species that were present in three or more years, removed instances in which a species was found only once at a given intertidal height (because intertidal height is used as a fixed effect in models; see below), and removed intertidal elevations that were sampled in fewer than 20 of the 40 sampled years. These strategies coarsened the resolution of our data, but allowed us to maximize the number of species included in our analysis. In total, we modeled changes in abundance over time for 26 species in the density group and 49 species in the percent cover group (Fig. S6, S7).

For the density group, we used gamma regressions with log links in the `brms` R package (Bürkner, 2017) to calculate abundance change over time, with a fixed categorical effect of intertidal elevation to control for initial differences in density across the intertidal zone. We extracted the log-linked fixed effect coefficient for “year” for each species, representing the change in abundance through time. In order to run gamma regressions, we changed zeros in the dataset to 0.01, consistent with the assumption that species have low densities undetectable at the sampled resolution. As a sensitivity test, we also ran analyses with log-linked Tweedie regressions with the `glmmTMB` R package (Brooks et al., 2017), which, unlike gamma regressions, allow for zero values and zero-inflated data; while some species’ coefficients changed using Tweedie models (with two of 26 coefficients switching signs), the relationship between abundance change and thermal affinity did not (Fig. S8).

For the percent cover group, we used ordered beta regressions (Kubinec, 2023), which combine beta regressions with ordered logit models to describe trends over continuous scales with upper and lower bounds (here, 0 and 100) using the `ordbetareg` R package (Kubinec, 2023), which similarly uses `brms` internally. We again modeled abundance (percent cover) across years with a fixed categorical effect for shore level.

To test whether thermal affinity predicted abundance change on Appledore Island, we matched abundance change coefficients from the above models with occupancy-derived thermal affinities for each species (matching 26 of 26 species in the density group and 48 of 49 species in the percent cover group) and used linear regressions to predict the coefficients of abundance change by the (mean) thermal affinities of species. Regression model assumption checks are shown in Fig. S9. Because the two types of abundance change models produce coefficients with different links (log linked gamma regressions for density species and logit linked ordered beta regressions for percent cover), the coefficient values are difficult to directly compare, as are their respective relationships with thermal affinity. However, seven species were documented in both datasets—measured sometimes as density counts and sometimes as percent cover throughout the sampling period—which allowed us to conduct a sensitivity test to check the consistency of trends produced by the two modeling methods. Of these seven species, five had coefficients of abundance change with the same sign between the two modeling methods, and the relationships between thermal affinity and abundance change using only these seven species was significant and similar (even steeper) compared to using the full species lists (Fig S10). While we present relationships

between abundance change and mean thermal affinity in the main text, we additionally modeled abundance change coefficients as functions of species' thermal minima and maxima (Fig. S11).

Richness Shifts

We assessed changes in species richness on Appledore Island throughout the sampling period both as an overall trend, and across intertidal elevations over time. To assess overall richness change, we used the highly sampled dataset (to standardize sampling effort between transects and intertidal heights), and calculated the annual mean species richness summed across all intertidal heights in replicate quadrats (n = 1–4) within each transect. We used a linear model to model mean richness as a function of year, and included transect ID as an additive categorical term to control for richness differences between transects. Because we were primarily interested in identifying change in overall richness over time, we did not test additional models. We extracted the coefficient and *p*-value of the "year" term as change in overall richness across time (model assumptions checks in Fig. S12).

To calculate richness across intertidal heights, we used the full dataset (which spans a greater vertical breadth than the highly sampled dataset), but due to inconsistencies in the number of replicates, intertidal heights, and transects sampled per year, we averaged richness within each intertidal height and year across all transects (n = 1–17), each rarefied to the average richness value within the minimum number of replicates (n = 1). We included only quadrats that had a rarefied richness value greater than zero (excluding bare rock, for example). We tested multiple generalized linear models with a log-link and gamma distributions to find the best predictive fit of richness as a function of time and/or intertidal height using information theoretic approaches, some of which allowed for nonlinear effects of intertidal height on intertidal species richness (Zwerschke et al., 2013). We performed model selection using AICc values from all tested models to select the best model fit (Table S1). Our final model predicted mean quadrat richness as an interactive function of year and intertidal height as a quadratic term (Table S1). As a sensitivity test, we repeated this methodology with the highly sampled dataset (instead of the full dataset) and identified the same best-performing model and the same relationship of richness change across intertidal elevations and years (Fig. S13). Model assumptions for the depth-stratified richness model are shown in Fig. S14.

Community Temperature Index Shifts

We used occupancy-derived thermal affinities and species abundance data to test for changes in community temperature index (CTI), both on the island as a whole and across shore levels throughout the sampling period. CTI is normally calculated as the average of species' thermal affinities within a community, weighted by the relative abundance of species (Devictor et al., 2008). Here, we faced difficulty weighting the abundance of all species simultaneously since two different abundance metrics—density and percent cover—were used for different groups of species. Thus, we calculated CTI within the two sampling datasets (density and percent cover) independently, weighting by the respective abundance value in each, resulting in a dataset of two CTI values per year.

To assess island-wide CTI change, we used the highly sampled dataset to average the mean thermal affinities of all species across all transects in each year, weighted by their relative abundance (density or percent cover). We then conducted a linear regression, modeling CTI as a function of year, with an additive categorical variable for species group (density or percent cover group), extracting the coefficient for the year term as the change in CTI over time. Model assumptions are shown in Fig. S15.

To assess CTI changes across the intertidal height gradient, we again used the highly sampled dataset, but this time averaged the mean thermal affinities of all species present within each intertidal height, weighted by their relative abundance (density or percent cover). We tested multiple models to explain CTI as a function of time and intertidal height, allowing for both additive and interactive effects intertidal height and year, as well options including intertidal height as a quadratic term, and we included the dataset (density or percent cover) both as an additive and interactive categorical variable. We used AICc values to select the model of best fit. Our final model explained CTI as a function of time and an interactive effect of intertidal height and species group (Table S2). Model assumptions are shown in Fig. S16.

Results

Species Distribution Shifts

We identified 16 species that disappeared from the Appledore Island intertidal community, 18 species that arrived and persisted, 34 species that were persistent throughout the sampling period, and eight species with other patterns (Fig 2a,b), and we compared thermal affinities between each group. Global hypotheses of species redistributions suggest that species that arrived in the community should have higher thermal affinities than species that disappeared, and thus we were most interested in the comparison between these two groups. We found that the arriving species group had significantly higher mean thermal affinities than the disappearing species group (Fig. 2d), and that the arriving group had the highest thermal maxima, although this difference was only statistically significant when compared to the persistent group (Fig. 2e). We found no differences in thermal minima between groups (Fig. 2e). The arriving species group uniquely showed higher mean and maximum thermal affinities compared to the corresponding sea surface temperature variables on Appledore Island both at the start (1982) and by the end (2023) of the sampling period (Fig. 2c–e). We additionally identified 14 species in the dataset that were not native to the Gulf of Maine region (Fig. 2a,b). Of these non-native species, half were in the “arriving species” group, comprising 39% of all species that arrived and persisted in the study area throughout the sampling period (Fig. 2b).

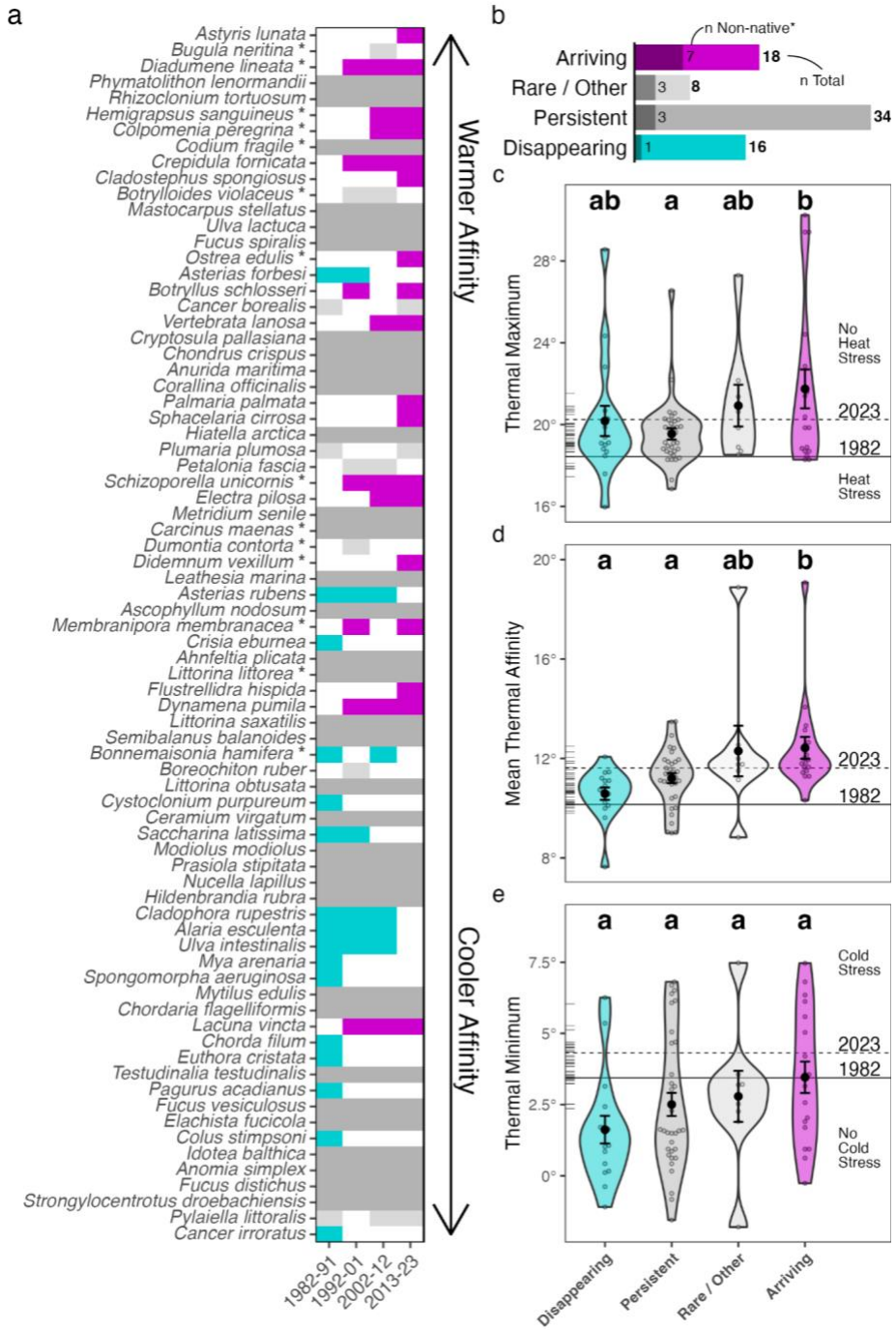

Figure 2. Thermal affinities of disappearing, persistent, rare, and arriving species in the Appledore Island intertidal community. (a) Species presences in the community in each 10-year sampling bin, arranged by (mean) thermal affinity. Species not native to the Gulf of Maine region are marked with an asterisk. (b) Total number and number of non-native species per occurrence group. (c–e) Thermal affinities of each species occurrence group using maximum, mean, and minimum monthly temperatures of global occurrences. Violins represent distributions of values for all species, points and error bars represent mean and SE. Letters indicate groups from ANOVA and Tukey post-hoc analyses. Tick marks along the y-axes show raw values of the corresponding temperature variable (hottest month, annual mean, and coldest month sea surface temperature) at Appledore Island in every year of the sampling span, and horizontal lines show the modelled temperature values at the start and end of the study period (solid and dashed line, 1982 and 2023). Colors in all plots represent the groups assigned to species by their presence patterns in (a): disappearing (turquoise), persistent (dark grey), rare/other (light grey), and arriving (magenta).

Most species did not show significant changes in vertical distributions over time. Only nine species out of 43 showed significant shifts in either direction (upwards or downwards) of any parameter measured from presences in the combined dataset (totaling 14 significant of 172 shifts, Fig. 3a). Of significant shifts from the combined dataset, downward shifts were slightly more common at the maximum occurrence height than were upward shifts, whereas mean, median, and minimum occurrence heights had more equal numbers of upwards and downwards shifts (Fig. 3a). Of all shifts in the combined dataset (significant and non-significant), downwards trends were more common at the maximum occurrence height (60%), whereas minimum occurrence heights more often had upwards trends (63%) (Fig. 3a). When assessing shifts in the density and percent cover datasets independently, percent cover species seem to exhibit stronger contrasts in shifts, with a higher proportion of upper distributional limits trending downwards and a higher proportion of lower limits trending upwards (Fig. 3b,c). When excluding species with distributions bordering margins of the sampling domain, these trends did not meaningfully change (Fig. S5). Full distributional data are presented in Fig. S4 and all model trends in Table S3.

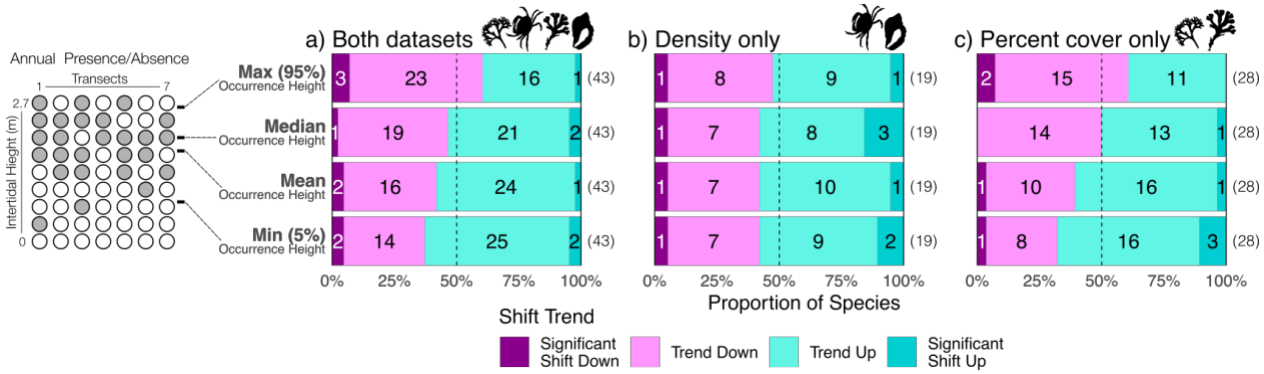

Figure 3. Shifts in individual species' vertical distributions throughout the sampling period at species' maximum (95th percentile) occurrences, mean, median, and minimum (5th percentile) occurrences in the intertidal zone. Downward shifts in pink and upward shifts in turquoise; dark colors show significant trends ($p < 0.05$). Plots show shifts for all species (a), species in the density dataset only (b), and species in the percent cover dataset only (c). Sample sizes are shown in parentheses. Note that sample sizes from (b) and (c) do not sum to (a), since here, four species are in both datasets and their shifts in (a) are calculated from presences in both datasets combined.

Abundance Change

Occupancy-derived mean thermal affinities for species in the density group ranged from 7.6 to 14.1°C, and log-linked coefficients of abundance change over years of sampling ranged from -0.121 to 0.177, or from approximately an 11% decrease per year to a 19% increase per year ($1 - e^{-0.121}$ and $e^{0.177} - 1$, respectively) (Fig. S6). In the percent cover group, mean thermal affinities

ranged from 8.8 to 14.1°C and logit-linked coefficients of change in percent cover ranged from -0.108 to 0.265 (Fig. S7).

In both groups, we found significant positive relationships between mean thermal affinity and coefficients of abundance change, such that species with warmer thermal affinities increased in abundance on Appledore Island throughout the sampling period, and species with cooler thermal affinities decreased in abundance (Fig. 4). Thermal affinity explained more of the variance around the mean in the density versus the percent cover group (Multiple R^2 = 0.40 for density; multiple R^2 = 0.14 for percent cover). We additionally modeled abundance change coefficients by other thermal traits (thermal maximum and thermal minimum), finding significant positive relationships between abundance change and thermal maxima for both groups and thermal minima for the percent cover group (Fig. S11).

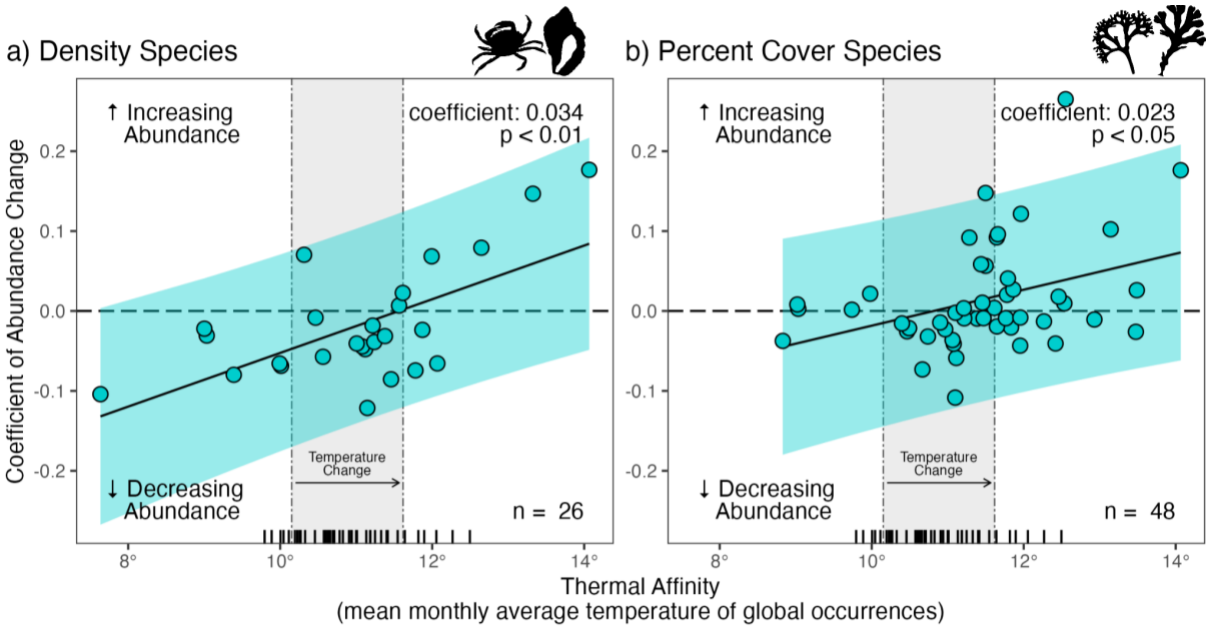

Figure 4. Mean thermal affinity and abundance change coefficients of species on Appledore Island. Trend lines show the relationship between mean thermal affinity (mean of annual mean temperatures of global occurrences) and the coefficient of abundance change over time on Appledore Island for species in the density group (a) and percent cover group (b). Blue shaded areas represent prediction intervals of the regression fits. Vertical grey boxes represent the fitted minimum and maximum values (1982 and 2023) of annual mean sea surface temperature on Appledore Island, and black ticks show the raw values of mean sea surface temperature in all years throughout the study period.

Richness Shifts

Overall, species richness within transects increased over the course of the sampling period, with a significant increase of about 0.5 species per decade (p < 0.01) (Fig. 5a). Across intertidal heights, we found a significant positive interaction between year and a quadratic term for intertidal

height, such that richness increased at lower intertidal heights and decreased at higher intertidal heights throughout the sampling period, with the highest rate of increase near chart datum (Fig. 5b).

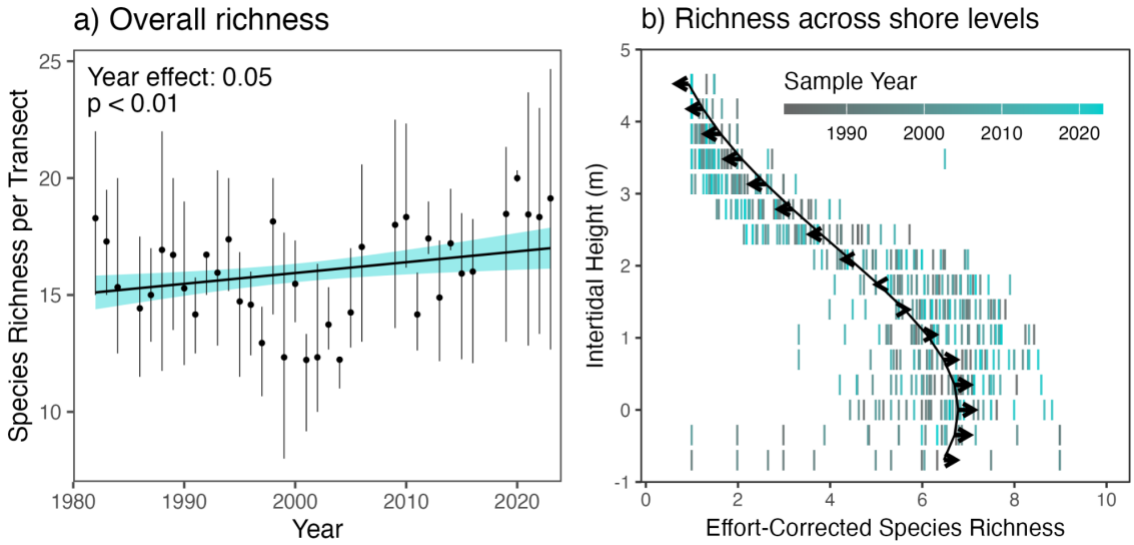

Figure 5. Species richness changes on Appledore Island as a whole (a) and across intertidal heights (b) over the 42-year sampling period. In (a), black line and blue shadow show the main effect and 95% confidence interval for the "year" term of the overall richness model using the highly sampled dataset. Points show mean richness between 7 transects, and bars show the 25th and 75th percentiles. In (b), colored dashes show the average species richness of communities in each sampling elevation, rarefied to one replicate quadrat. The curved line shows the model-predicted richness in the first year of sampling (1982), and arrows show the model-predicted trajectories of species richness across elevations throughout the sampling period.

Community Temperature Index Shifts

Whole-community CTI increased over time, with a rate of change of about 0.054 ± 0.021SE °C per decade (Fig. 6a). While the community appears to be shifting towards warmer-affinity species, this shift was almost seven times slower than the rate of temperature increase at the study location throughout the sampling period (mean annual temperature increase = 0.36°C/decade ± 0.06 SE, Fig. 6a, Fig. S1). Across intertidal heights, the best-fit model (Table S3) showed that CTI increased significantly over time at a consistent rate across intertidal elevations and between the two datasets (0.044 ± 0.009SE °C per decade, Fig. 6b). Differences in baseline CTI across intertidal heights showed opposing patterns between the two datasets (Fig. 6b), but the temporal trend was uniform.

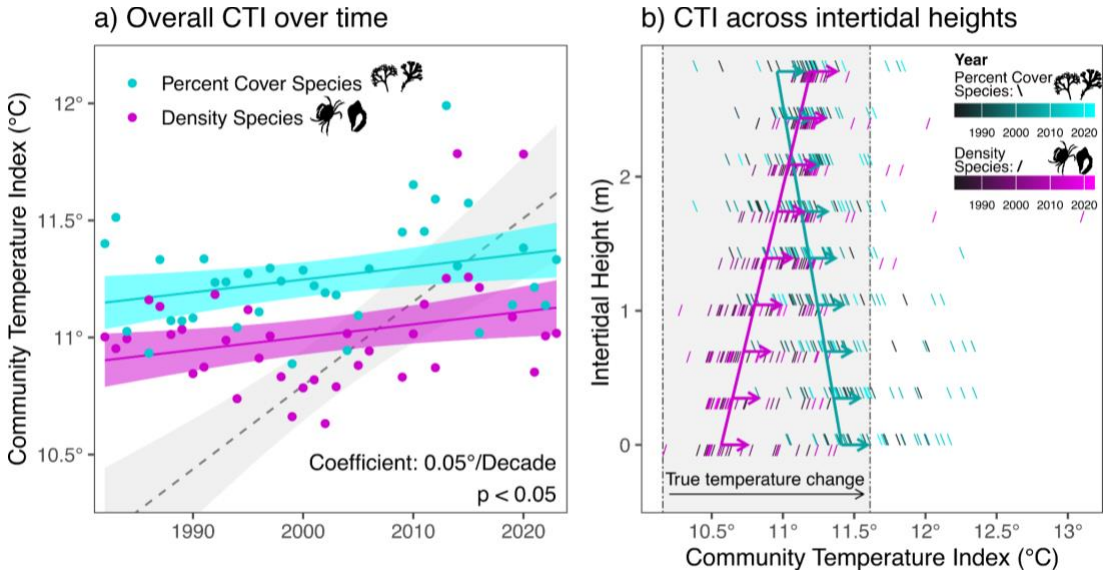

Figure 6. Community Temperature Index (CTI) change of the whole-island community (a) and stratified across intertidal elevations (b). In (a), solid lines and colored shadows show the model fit and prediction interval of linear models for CTI change. The grey shadow and dashed line show the model fit and confidence interval of mean sea surface temperature throughout the sampling period. In (b), colored dashes show the CTI within intertidal heights across years of sampling. Diagonal lines show the model fit from the first year (1982), and arrows show the predicted change through time to 2023. Vertical dashed lines show the model-fitted change in temperature from 1982 to 2023 in the region.

Discussion

Overall, we found broad support for the role of climate change in driving intertidal community structure over four decades on Appledore Island. Observed changes were largely consistent with expectations of climate-driven biodiversity change at macroecological scales, supporting six of our seven globally-informed hypotheses for local biodiversity change. Over the 42-year period, warm-affinity species arrived or increased, and cold-affinity species declined or disappeared (Figs. 2, 4), representing multiple stages of predictable temperature-linked inbound and outbound range shifts occurring for species in the community (Bates et al., 2014). CTI shifted towards warmer-affinity species, both overall and across tidal elevations, indicating that thermophilization is occurring in the region (Fig. 6). Finally, increases in overall species richness are consistent with the expectation that warming is shifting richness peaks away from the equator towards temperate zones (Chaudhary et al., 2021), and the contrasting pattern of richness increasing in the low intertidal zone and decreasing in the high intertidal zone support the hypothesis that species could be responding to increasing thermal stress by shifting downwards (Fig. 5). These findings were globally coherent, and robust to several sensitivity tests that we conducted (Fig. S8, S10, S11, S13).

Despite this broad support for our hypotheses, we were largely unable to detect absolute vertical distribution shifts for most species (Fig. 3, S5). While this detection failure might be attributed to our limited sampling resolution over the vertical gradient (nine discrete intertidal heights within the highly sampled dataset), it might also demonstrate that absolute vertical distributions are not changing. Instead, within-range abundance changes or "leans" of species' distributions (Lenoir & Svenning, 2013) could be occurring—for example, as a result of altered recruitment dynamics (Petraitis & Dudgeon, 2020)—and subsequently driving community-level changes (Antão et al., 2022). Regardless, this contrast demonstrates that community-level metrics can be more sensitive indicators of change than species range limits, given limits in data resolution.

Species-level Changes

Assuming that thermal preferences and limitations drive latitudinal distributions of species (Sunday et al., 2012), we expected that warm-affinity species would appear in the community and cool-affinity species would disappear from the community over time as their ranges shift towards and away from Appledore Island, respectively. Because our biodiversity data revealed the outcomes of species in the local community over time (Fig. 2A), we used post-hoc analyses to test for differences between response-based groups. Indeed, we found that species that disappeared from the community over the 40-year period had significantly colder mean thermal affinities compared to species that appeared and persisted (Fig. 2c). These differences in mean thermal affinities indicate that species appearances and disappearances likely reflect either absolute or within-range distribution shifts across latitudes near trailing and leading range edges, respectively, with Appledore Island representing a cross-section of species' latitudinal ranges. Despite the more direct links of species' thermal minima and maxima to their survival, we found that mean thermal affinity was more predictive than thermal maximum or thermal minimum, which displayed fewer differences between response-based groups (Fig. 2c,e). Although mean temperature affinities support a thermally-linked basis for occurrence changes on Appledore Island, temperature does not explain everything. For example, species in the disappearing group did not significantly differ in thermal affinity by any metric from species in the persistent group, despite their different responses (Fig. 2c–e); assuming that the persistent group has therefore experienced similar thermal stress over the study span, additional factors such as behavioral adaptation, body form, or trophic level might explain why these species persisted instead of disappeared.

Comparing the thermal affinity metrics (maximum, mean, and minimum) to experienced temperatures on Appledore Island lends further support to temperature as a driver of species' responses. Warmest month, annual mean, and coldest month sea surface temperatures all increased, on average, at the study site throughout the study duration (Fig. S1). In many cases, thermal conditions switched from values below species' thermal limits/affinities at the start of the study period (1982) to values above the species' thermal limits/affinities by the end of the study period (2023) (Fig. 2c-e, horizontal lines). For example, Appledore Island's mean water temperatures were below the global-occurrence mean temperatures for 84% of all species in 1982, but for only 39% of all species in 2023 (Fig. 2d). Similarly, the warmest month temperature on Appledore Island surpassed the global 95th percentile warmest-month temperature thresholds for 68% of all species by 2023. Put more simply, as of 2023, Appledore Island is in the hottest 5% of global environments for the majority of its species (Fig. 2d). In contrast, most species—even at the start of the sampling period when temperatures were coolest—had thermal minima lower than coldest-month temperatures on Appledore Island (Fig. 2e) and were therefore not likely limited by cold stress, which further decreased over time as coldest-month temperatures rose. Only the arriving species group had an average thermal minimum exceeding the model-fitted coldest month temperature on Appledore Island at the start of the study period (mean thermal minimum = 3.46°C vs. model-fitted coldest month = 3.44°C, Fig. 2e). Coldest-month temperatures may have therefore prevented the survival of these species at the start of the sampling period, but warming allowed their establishment throughout the following four decades.

In addition to these broad-scale effects, we expected warming to affect species' distributions on a local scale by shifting species towards lower, more thermally benign intertidal heights, as has been observed and anticipated by others (Hansen, 2024; Harley, 2011; Harley & Paine, 2009; Sorte et al., 2019). However, we were unable to detect significant vertical shifts for most species using any distributional parameter (maximum, mean, median, minimum occurrence height, Fig. 3), likely owing to the inconsistency of the sampling design and the coarseness of species occurrence data across intertidal heights. Still, interpreting the nonsignificant directional trends can provide some insight into species' responses. We observed that species' maximum intertidal heights more often trended downwards (Fig. 3, S4, S5), consistent with the hypothesis that intensifying thermal and desiccation stress should limit upper distributions of species (Harley, 2011). In contrast, we observed that species' mean, median, and minimum distributional limits more often trended upwards (Fig. 3, S4, S5). While counterintuitive, these upward trends in lower distributional limits could still be indirect responses to temperature change. Because lower

intertidal limits are generally determined by biological pressures of predation and competition instead of environmental limitations (Connell, 1972), upward trends in these lower distributional limits could indicate increased predation pressure in the lower intertidal zone, possibly related to increased consumption requirements for resident predator species in warmer waters (Csik et al., 2023; Sanford, 2002). These contrasting trends were most apparent for species in our percent cover dataset (Fig. 3c, S5c). Given that these species are generally sessile and unable to regulate their position across intertidal elevations, their responses might indicate the direct and indirect climate pressures at opposite sides of their vertical distributions. Meanwhile, species in the density dataset, which are more mobile, did not have the same downward trend at the upper distribution limit (Fig. 3b, S5b), and could be behaviorally adapting to intensifying temperatures at the upper edge of their ranges by seeking out nearby thermal refugia (Virgin et al., 2025).

We related changes in the abundance of intertidal species on Appledore Island to their thermal affinities, hypothesizing that warmer-affinity species would increase and cooler-affinity species would decrease in abundance. As expected, we found significant positive relationships between abundance change and thermal affinity, in agreement with comparable studies (Sato et al., 2025), albeit with substantial variation around model fits. In both datasets, we observed clusters of species that had thermal affinities around 11°C (over half of species in both the density and percent cover datasets), which aligned closely with the mean sea surface temperature on Appledore Island throughout the sampling period (10.2°C to 11.6°C, fitted mean temperature values in 1982 and 2023). This alignment indicates that most species are indeed thermally adapted to this environment, but even these species—which are unlikely to be directly limited by temperatures in this range—sometimes increased or decreased in abundance much more than our models predicted. This variation suggests that direct temperature effects were not the only driver of species' abundances during the sampling period. Temperature-independent ecological factors or indirect temperature effects via competitive dynamics, increased predation risk, or cascading effects from changes to foundation species might instead explain abundance changes of these thermally-adapted species (Firth et al., 2009; Miller et al., 2014; Sorte et al., 2017).

For both occupancy and abundance changes, we found species' occupancy-derived mean affinities to be better predictors of observed changes than species' occupancy-derived thermal minima or maxima (Fig. 2c–e, Fig. S11). While mechanisms for predictive power of mean affinities are less clear, we expect that they performed better for three reasons. First, occupancy-derived minima and maxima are more likely to be influenced by sampling bias: if occurrence records do

not exist at the extremes of species' distributions, minima and maxima will be inaccurate, but means might still capture a representative value. Second, occupancy-derived thermal minima and maxima, even when accurately sampled, might not represent their true thermal tolerance limits, since species can underfill their potential thermal ranges for many reasons (Moore et al., 2023). Third, we calculated all thermal affinity metrics using sea surface temperature, which serves as a general predictor, but does not accurately reflect the seasonal extreme air temperatures experienced by intertidal organisms during emersion at low tide. Thus, our calculated thermal minima and maxima derived from sea surface temperatures likely underestimate the extremity of the true minimum and maximum body temperatures that intertidal species experience (Helmuth, 1998).

Community-Level Changes

Changes in the distribution and abundance of species on Appledore Island had ramifications at the community level that are consistent with expectations based on global trends and ecological dynamics in intertidal systems. We hypothesized that Appledore Island would increase in richness over time, assuming that the latitudinal biodiversity gradient is shifting away from the equator (Chaudhary et al., 2021). Although there is lively discussion regarding the weaker strength of the latitudinal biodiversity gradient in intertidal ecosystems compared to terrestrial or marine (Thyrring & Harley, 2024), we found that this rapidly-warming temperate site increased in overall richness by about 0.5 species per decade, or roughly a 13% increase across the 42-year period (Fig. 5). The high proportional contribution of non-native species to richness increases could harmonize these patterns: even if the latitudinal biodiversity gradient is weak in an "unaltered" natural state, the combination of shifting native species and species introductions result in increased richness with warming. Here, we cannot distinguish whether non-native species were introduced directly into the Gulf of Maine system during the sampling period or if they entered following introductions to nearby regions; regardless, the result was an increase in richness throughout the sampling span.

We also observed nonlinear changes in richness across the intertidal zone that supported, but slightly differed from our original hypothesis. We hypothesized that richness change would increase linearly from high to low intertidal elevations, with negative changes in the high intertidal zone and positive changes in the low intertidal zone. Instead, we found that both the initial pattern of richness across intertidal elevations and its change over time were nonlinear, with the best fit

model predicting richness as an interacting function of year and a quadratic term for intertidal elevation (Table S1). Over the sampling span, richness decreased in the high intertidal and increased in the mid-low intertidal up to a maximum near chart datum, below which the rate of richness increase slowed (Fig. 5b). While this pattern differed from our initial expectations, it is consistent with hypothesized drivers of vertical limits across intertidal heights. Because environmental stresses encountered during emersion (e.g., desiccation, temperature) often set the upper limit of intertidal species (Connell, 1961; Harley & Helmuth, 2003; Wethey, 1983), increasing temperatures could be shifting species to lower intertidal heights either by migration down shore for motile species or localized extirpation due to mortality high on shore. Alternatively, lower limits are typically set by biological constraints such as competition or predation pressure (Connell, 1972; Harley, 2011). The nonlinear increases in species richness that we observed across intertidal heights could be due to the interaction of such factors, whereby species have shifted down shore as a result of increasing climate stress, but are ultimately bound at their lower limits by competitive dominants and predator populations.

Overall and across intertidal heights, we observed shifts towards warmer-affinity communities per the CTI. While CTI cannot always be expected to scale linearly with community turnover (Flanagan et al., 2019) and might have drivers other than changing temperature (Bowler et al., 2017), its unit (°C) enables direct comparison between biological and environmental change within an ecosystem. The overall intertidal community increased in thermal index by 0.054 °C per decade, resulting in a 0.226°C increase over the 42-year span (Fig. 6a). While this increase was statistically significant, it was much slower than the rate at which mean annual sea surface temperature changed (0.357°C per decade, or 1.464°C over the 42-year span). In other words, CTI increased about 6.5 times more slowly than the mean annual temperature (0.15°C CTI for every 1°C temperature change). Slow CTI responses compared to temperature changes are not uncommon across ecological communities (Bertrand et al., 2011; Devictor et al., 2008; Lehikoinen et al., 2021; Richard et al., 2021; Rosenblad et al., 2023), but the delay-ratio we observe here (0.15) is smaller than most, likely owing to the fast rate of temperature change in this region, the slow response of the biological community, or both. When stratified across intertidal elevation, CTI increased even more slowly (0.044°C/decade, Fig. 6b) but consistently across intertidal elevations, as we hypothesized. One surprise was the contrasting initial trends of CTI across intertidal heights between species groups. We expected both communities to exhibit increasing CTI with increasing intertidal elevations, with the high intertidal communities having the highest thermal affinities (Fig. 1); the percent cover group, however, showed the opposite trend (Fig 6b).

Appearances of invasive and/or southern-affinity macroalgae in the subtidal zone are well-documented in this region, and could explain this counterintuitive pattern (Dijkstra et al., 2017).

Increasing Vulnerability of the Intertidal Community

Together, our analyses reveal several indications of increased climate risk to the Appledore Island intertidal community that accumulated throughout the duration of our study. Our species-specific analyses showed that by the end of the study period, the annual mean and warmest-month sea surface temperatures were warmer than the mean and maximum affinities of the majority of species in the community (Fig. 2c-d, 4, S11), indicating the shrinking or disappearance of thermal safety margins, which could lead to further decline or extirpation of local populations (Vinagre et al., 2019). Although occupancy-derived mean thermal affinity might not exactly estimate the optimal temperature of performance (Martin & Huey, 2008), annual mean sea surface temperatures now exceeding these mean affinities might push species closer to sharp declines in performance, which are generally thought to follow optimum temperature peaks along thermal performance curves (Malusare et al., 2023). These organisms, now living closer to their thermal maxima, will be more sensitive to both gradual warming and short-term thermal variability, including heatwaves, which are becoming longer and more frequent as a result of climate change (Oliver et al., 2018; Perkins-Kirkpatrick & Lewis, 2020; Vasseur et al., 2014).

Our community-level analyses revealed similar vulnerabilities; CTI of the Appledore Island intertidal community began from an initial positive bias at the start of the sampling period and switched to a negative bias sometime in the 2010s as the rate of temperature warming exceeded the rate of CTI change (Fig 6a). This newfound negative bias threatens the stability of the ecological community if climate warming continues at its current rate (Stuart-Smith et al., 2015). Across depths, we show that species in our density group (mostly motile invertebrates) inhabiting the lower intertidal zone are particularly negatively-biased, and might already rely on strategies such as sheltering under canopy macroalgae during low tide to survive in the current “too-warm” conditions (Burrows et al., 2020). If these interactions are necessary or beneficial for the survival of motile organisms, then the community might additionally be at risk of cascading effects if other stressors such as storm events remove macroalgae or other “leverage” species (Kroeker & Sanford, 2022).

Conclusion

Our work demonstrates how data collected over long timeframes in a single location—in our case, from undergraduate surveys at a university marine laboratory—can be globally contextualized in order to assess larger-scale biodiversity responses to climate change. Context-informed fixed-location species' responses have helped reveal large-scale patterns since some of the earliest evidence of climate-driven range shifts (Barry et al., 1995) and can lend even more credence to large-scale trends when temporal trends from multiple sites are combined (Hastings et al., 2020). Given that datasets of similar quality and resolution likely exist at other university-affiliated field stations, our approach is pragmatic; identifying temporal trends from other such locations using methods similar to ours, and comparing patterns between locations could help to fill knowledge gaps in species' or community responses to climate change where consistent spatio-temporal surveys are not available. Our elevation-stratified analyses also show that community-level metrics can change even in the absence of absolute species-specific vertical distribution shifts, indicating that within-range abundance changes can still substantially affect community structure (Antão et al., 2022). This lesson can be extrapolated to community predictions, which often focus on the arrival and disappearance of species to quantify community changes, but might miss substantial variation by ignoring within-range abundance changes. Our results provide evidence that predictable climate-driven change is observable in intertidal systems, and lend strong support to temperature change as a driver of species' abundances and community compositions.

Supplementary Information

Supplementary Figures S1-S16 and Supplementary Tables S1-S3 are available online

Acknowledgements

This research is a product of a Living Data Project working group funded by the Canadian Institute of Ecology and Evolution and a Natural Sciences and Engineering Research Council CREATE grant. JL received additional support for this work, including a Doctoral Research Grant from Fonds du Recherche du Quebec (FRQNT) (https://doi.org/10.69777/297888) and a Réal-Decoste Excellence Scholarship from FRQNT and Ouranos Inc (https://doi.org/10.69777/371714). JAD, JEKB, and KB were supported to curate and explore long-term data from the Shoals Marine Lab

by the Regional Association for Research in the Gulf of Maine. This manuscript is Shoals Marine Laboratory Contribution number 215.

Works Cited

Antão, L. H., Weigel, B., Strona, G., Hällfors, M., Kaarlejärvi, E., Dallas, T., Opedal, Ø. H., Heliölä, J., Henttonen, H., Huitu, O., Korpimäki, E., Kuussaari, M., Lehikoinen, A., Leinonen, R., Lindén, A., Merilä, P., Pietiäinen, H., Pöyry, J., Salemaa, M., … Laine, A.-L. (2022). Climate change reshuffles northern species within their niches. *Nature Climate Change*, *12*(6), 587–592. https://doi.org/10.1038/s41558-022-01381-x

Barry, J. P., Baxter, C. H., Sagarin, R. D., & Gilman, S. E. (1995). Climate-related, long-term faunal changes in a california rocky intertidal community. *Science*, *267*(5198), 672–675. https://doi.org/10.1126/science.267.5198.672

Bates, A. E., Pecl, G. T., Frusher, S., Hobday, A. J., Wernberg, T., Smale, D. A., Sunday, J. M., Hill, N. A., Dulvy, N. K., Colwell, R. K., Holbrook, N. J., Fulton, E. A., Slawinski, D., Feng, M., Edgar, G. J., Radford, B. T., Thompson, P. A., & Watson, R. A. (2014). Defining and observing stages of climate-mediated range shifts in marine systems. *Global Environmental Change*, *26*, 27–38. https://doi.org/10.1016/j.gloenvcha.2014.03.009

Bertrand, R., Lenoir, J., Piedallu, C., Riofrío-Dillon, G., de Ruffray, P., Vidal, C., Pierrat, J.-C., & Gégout, J.-C. (2011). Changes in plant community composition lag behind climate warming in lowland forests. *Nature*, *479*(7374), Article 7374. https://doi.org/10.1038/nature10548

Billman, P. D., Carroll, K. A., Schleicher, D. J., & Freeman, B. G. (2025). Forecasting range shifts using abundance distributions along environmental gradients. *Frontiers in Ecology and the Environment*, *23*(4), e2820. https://doi.org/10.1002/fee.2820

Blouin, N. A., Brodie, J. A., Grossman, A. C., Xu, P., & Brawley, S. H. (2011). Porphyra: A marine crop shaped by stress. *Trends in Plant Science*, *16*(1), 29–37. https://doi.org/10.1016/j.tplants.2010.10.004

759 Bowler, D. E., Hof, C., Haase, P., Kröncke, I., Schweiger, O., Adrian, R., Baert, L., Bauer, H.-G.,
760 Blick, T., Brooker, R. W., Dekoninck, W., Domisch, S., Eckmann, R., Hendrickx, F.,
761 Hickler, T., Klotz, S., Kraberg, A., Kühn, I., Matesanz, S., … Böhning-Gaese, K. (2017).
762 Cross-realm assessment of climate change impacts on species' abundance trends.
763 *Nature Ecology & Evolution*, *1*(3), Article 3. https://doi.org/10.1038/s41559-016-0067
764 Brooks, M., E., Kristensen, K., Benthem, K., J. ,van, Magnusson, A., Berg, C., W., Nielsen, A.,
765 Skaug, H., J., Mächler, M., & Bolker, B., M. (2017). glmmTMB balances speed and
766 flexibility among packages for zero-inflated generalized linear mixed modeling. *The R*
767 *Journal*, *9*(2), 378. https://doi.org/10.32614/RJ-2017-066
768 Bürkner, P.-C. (2017). **brms**: An *R* package for bayesian multilevel models using *stan*. *Journal*
769 *of Statistical Software*, *80*(1). https://doi.org/10.18637/jss.v080.i01
770 Burrows, M. T., Hawkins, S. J., Moore, J. J., Adams, L., Sugden, H., Firth, L., & Mieszkowska,
771 N. (2020). Global-scale species distributions predict temperature-related changes in
772 species composition of rocky shore communities in Britain. *Global Change Biology*,
773 *26*(4), 2093–2105. https://doi.org/10.1111/gcb.14968
774 Chaudhary, C., Richardson, A. J., Schoeman, D. S., & Costello, M. J. (2021). Global warming is
775 causing a more pronounced dip in marine species richness around the equator.
776 *Proceedings of the National Academy of Sciences*, *118*(15), e2015094118.
777 https://doi.org/10.1073/pnas.2015094118
778 Comte, L., Grenouillet, G., Bertrand, R., Murienne, J., Bourgeaud, L., Hattab, T., & Lenoir, J.
779 (2020). *BioShifts: A global geodatabase of climate-induced species redistribution over*
780 *land and sea* (p. 5238495 Bytes) [Dataset]. figshare.
781 https://doi.org/10.6084/M9.FIGSHARE.7413365.V1
782 Connell, J. H. (1961). The influence of interspecific competition and other factors on the
783 distribution of the barnacle *Chthamalus stellatus*. *Ecology*, *42*(4), 710–723.
784 https://doi.org/10.2307/1933500

785 Connell, J. H. (1972). Community Interactions on Marine Rocky Intertidal Shores. *Annual*
786 *Review of Ecology and Systematics*, *3*(1), 169–192.
787 https://doi.org/10.1146/annurev.es.03.110172.001125
788 Csik, S. R., DiFiore, B. P., Kraskura, K., Hardison, E. A., Curtis, J. S., Eliason, E. J., & Stier, A.
789 C. (2023). The metabolic underpinnings of temperature-dependent predation in a key
790 marine predator. *Frontiers in Marine Science*, *10*, 1072807.
791 https://doi.org/10.3389/fmars.2023.1072807
792 Day, P. B., Stuart-Smith, R. D., Edgar, G. J., & Bates, A. E. (2018). Species' thermal ranges
793 predict changes in reef fish community structure during 8 years of extreme temperature
794 variation. *Diversity and Distributions*, *24*(8), 1036–1046.
795 https://doi.org/10.1111/ddi.12753
796 Devictor, V., Julliard, R., Couvet, D., & Jiguet, F. (2008). Birds are tracking climate warming, but
797 not fast enough. *Proceedings of the Royal Society B: Biological Sciences*, *275*(1652),
798 2743–2748. https://doi.org/10.1098/rspb.2008.0878
799 Dijkstra, J. A., Harris, L. G., Mello, K., Litterer, A., Wells, C., & Ware, C. (2017). Invasive
800 seaweeds transform habitat structure and increase biodiversity of associated species.
801 *Journal of Ecology*, *105*(6), 1668–1678. https://doi.org/10.1111/1365-2745.12775
802 Drake, M. J., Miller, N. A., & Todgham, A. E. (2017). The role of stochastic thermal
803 environments in modulating the thermal physiology of an intertidal limpet, *Lottia digitalis*.
804 *Journal of Experimental Biology*, *220*(17), 3072–3083.
805 https://doi.org/10.1242/jeb.159020
806 Fenberg, P. B., & Rivadeneira, M. M. (2011). Range limits and geographic patterns of
807 abundance of the rocky intertidal owl limpet, *Lottia gigantea*. *Journal of Biogeography*,
808 *38*(12), 2286–2298. https://doi.org/10.1111/j.1365-2699.2011.02572.x
809 Firth, L. B., Crowe, T. P., Moore, P., Thompson, R. C., & Hawkins, S. J. (2009). Predicting
810 impacts of climate-induced range expansion: An experimental framework and a test

involving key grazers on temperate rocky shores. *Global Change Biology*, *15*(6), 1413–1422. https://doi.org/10.1111/j.1365-2486.2009.01863.x

Flanagan, P. H., Jensen, O. P., Morley, J. W., & Pinsky, M. L. (2019). Response of marine communities to local temperature changes. *Ecography*, *42*(1), 214–224. https://doi.org/10.1111/ecog.03961

García Molinos, J., Burrows, M. T., & Poloczanska, E. S. (2017). Ocean currents modify the coupling between climate change and biogeographical shifts. *Scientific Reports*, *7*(1), Article 1. https://doi.org/10.1038/s41598-017-01309-y

Givan, O., Edelist, D., Sonin, O., & Belmaker, J. (2018). Thermal affinity as the dominant factor changing Mediterranean fish abundances. *Global Change Biology*, *24*(1). https://doi.org/10.1111/gcb.13835

Hansen, R. (2024). *New lows: The effects of climate change-associated warming on vertical distributions of rocky intertidal communities* [PhD Thesis, University of British Columbia]. https://doi.library.ubc.ca/10.14288/1.0441344

Harley, C. D. G. (2011). Climate change, keystone predation, and biodiversity loss. *Science*, *334*(6059), 1124–1127. https://doi.org/10.1126/science.1210199

Harley, C. D. G., & Helmuth, B. (2003). Local- and regional-scale effects of wave exposure, thermal stress, and absolute versus effective shore level on patterns of intertidal zonation. *Limnology and Oceanography*, *48*(4), 1498–1508. https://doi.org/10.4319/lo.2003.48.4.1498

Harley, C. D. G., & Paine, R. T. (2009). Contingencies and compounded rare perturbations dictate sudden distributional shifts during periods of gradual climate change. *Proceedings of the National Academy of Sciences*, *106*(27), 11172–11176. https://doi.org/10.1073/pnas.0904946106

835 Hastings, R. A., Rutterford, L. A., Freer, J. J., Collins, R. A., Simpson, S. D., & Genner, M. J.
836 (2020). Climate change drives poleward increases and equatorward declines in marine
837 species. *Current Biology*, *30*(8), 1572-1577.e2. https://doi.org/10.1016/j.cub.2020.02.043
838 Helmuth, B. (1998). Intertidal mussel microclimates: Predicting the body temperature of a
839 sessile invertebrate. *Ecological Monographs*, *68*(1), 51–74. https://doi.org/10.1890/0012-
840 9615(1998)068%255B0051:IMMPTB%255D2.0.CO;2
841 Helmuth, B., Broitman, B. R., Blanchette, C. A., Gilman, S., Halpin, P., Harley, C. D. G.,
842 O'Donnell, M. J., Hofmann, G. E., Menge, B., & Strickland, D. (2006). Mosaic patterns of
843 thermal stress in the rocky intertidal zone: Implications for climate change. *Ecological*
844 *Monographs*, *76*(4), 461–479. https://doi.org/10.1890/0012-
845 9615(2006)076%255B0461:MPOTSI%255D2.0.CO;2
846 Helmuth, B., Harley, C. D. G., Halpin, P. M., O'Donnell, M., Hofmann, G. E., & Blanchette, C. A.
847 (2002). Climate Change and Latitudinal Patterns of Intertidal Thermal Stress. *Science*,
848 *298*(5595), 1015–1017. https://doi.org/10.1126/science.1076814
849 Helmuth, B., & Hofmann, G. E. (2001). Microhabitats, thermal heterogeneity, and patterns of
850 physiological stress in the rocky intertidal zone. *The Biological Bulletin*, *201*(3), 374–384.
851 https://doi.org/10.2307/1543615
852 Jones, S. J., Southward, A. J., & Wethey, D. S. (2012). Climate change and historical
853 biogeography of the barnacle *Semibalanus balanoides*. *Global Ecology and*
854 *Biogeography*, *21*(7), 716–724. https://doi.org/10.1111/j.1466-8238.2011.00721.x
855 Kroeker, K. J., & Sanford, E. (2022). Ecological leverage points: Species interactions amplify the
856 physiological effects of global environmental change in the ocean. *Annual Review of*
857 *Marine Science*, *14*(1), 75–103. https://doi.org/10.1146/annurev-marine-042021-051211
858 Krumhansl, K. A., Brooks, C. M., Lowen, J. B., O'Brien, J. M., Wong, M. C., & DiBacco, C.
859 (2024). Loss, resilience and recovery of kelp forests in a region of rapid ocean warming.
860 *Annals of Botany*, *133*(1), 73–92. https://doi.org/10.1093/aob/mcad170

Krumhansl, K. A., Gentleman, W., Lee, K., Ramey-Balci, P., Goodwin, J., Wang, Z., Lowen, B., Lyons, D., Therriault, T. W., & DiBacco, C. (2023). Permeability of coastal biogeographic barriers to marine larval dispersal on the east and west coasts of North America. *Global Ecology and Biogeography*, *32*(6), 945–961. https://doi.org/10.1111/geb.13654

Kubinec, R. (2023). Ordered Beta Regression: A Parsimonious, Well-Fitting Model for Continuous Data with Lower and Upper Bounds. *Political Analysis*, *31*(4), 519–536. https://doi.org/10.1017/pan.2022.20

Lawlor, J. A., Comte, L., Grenouillet, G., Lenoir, J., Baecher, J. A., Bandara, R. M. W. J., Bertrand, R., Chen, I.-C., Diamond, S. E., Lancaster, L. T., Moore, N., Murienne, J., Oliveira, B. F., Pecl, G. T., Pinsky, M. L., Rolland, J., Rubenstein, M., Scheffers, B. R., Thompson, L. M., … Sunday, J. (2024). Mechanisms, detection and impacts of species redistributions under climate change. *Nature Reviews Earth & Environment*, *5*(5), 351–368. https://doi.org/10.1038/s43017-024-00527-z

Lehikoinen, A., Lindström, Å., Santangeli, A., Sirkiä, P. M., Brotons, L., Devictor, V., Elts, J., Foppen, R. P. B., Heldbjerg, H., Herrando, S., Herremans, M., Hudson, M. R., Jiguet, F., Johnston, A., Lorrilliere, R., Marjakangas, E., Michel, N. L., Moshøj, C. M., Nellis, R., … Van Turnhout, C. (2021). Wintering bird communities are tracking climate change faster than breeding communities. *Journal of Animal Ecology*, *90*(5), 1085–1095. https://doi.org/10.1111/1365-2656.13433

Lenoir, J., Bertrand, R., Comte, L., Bourgeaud, L., Hattab, T., Murienne, J., & Grenouillet, G. (2020). Species better track climate warming in the oceans than on land. *Nature Ecology & Evolution*, *4*(8), Article 8. https://doi.org/10.1038/s41559-020-1198-2

Lenoir, J., & Svenning, J.-C. (2013). Latitudinal and Elevational Range Shifts under Contemporary Climate Change. In *Encyclopedia of Biodiversity* (pp. 599–611). Elsevier. https://doi.org/10.1016/B978-0-12-384719-5.00375-0

886 Malusare, S. P., Zilio, G., & Fronhofer, E. A. (2023). Evolution of thermal performance curves: A
887 meta-analysis of selection experiments. *Journal of Evolutionary Biology*, *36*(1), 15–28.
888 https://doi.org/10.1111/jeb.14087
889 Mannion, P. D., Upchurch, P., Benson, R. B. J., & Goswami, A. (2014). The latitudinal
890 biodiversity gradient through deep time. *Trends in Ecology & Evolution*, *29*(1), 42–50.
891 https://doi.org/10.1016/j.tree.2013.09.012
892 Martin, T. L., & Huey, R. B. (2008). Why "suboptimal" is optimal: Jensen's Inequality and
893 ectotherm thermal preferences. *The American Naturalist*, *171*(3), E102–E118.
894 https://doi.org/10.1086/527502
895 Mieszkowska, N. (2016). Intertidal indicators of climate and global change. In *Climate Change*
896 (pp. 213–229). Elsevier. https://doi.org/10.1016/B978-0-444-63524-2.00014-2
897 Mieszkowska, N. (2025). Evidence of climate change (intertidal indicators). In *Energy and*
898 *Climate Change* (pp. 43–66). Elsevier. https://doi.org/10.1016/B978-0-443-21927-
899 6.00024-6
900 Mieszkowska, N., Burrows, M. T., Hawkins, S. J., & Sugden, H. (2021). Impacts of pervasive
901 climate change and extreme events on rocky intertidal communities: Evidence from long-
902 term data. *Frontiers in Marine Science*, *8*, 642764.
903 https://doi.org/10.3389/fmars.2021.642764
904 Miller, L. P., Matassa, C. M., & Trussell, G. C. (2014). Climate change enhances the negative
905 effects of predation risk on an intermediate consumer. *Global Change Biology*, *20*(12),
906 3834–3844. https://doi.org/10.1111/gcb.12639
907 Moore, N. A., Morales-Castilla, I., Hargreaves, A. L., Olalla-Tárraga, M. Á., Villalobos, F., Calosi,
908 P., Clusella-Trullas, S., Rubalcaba, J. G., Algar, A. C., Martínez, B., Rodríguez, L.,
909 Gravel, S., Bennett, J. M., Vega, G. C., Rahbek, C., Araújo, M. B., Bernhardt, J. R., &
910 Sunday, J. M. (2023). Temperate species underfill their tropical thermal potentials on

land. *Nature Ecology & Evolution*, *7*(12), 1993–2003. https://doi.org/10.1038/s41559-023-02239-x

OBIS. (2025). *Ocean Biodiversity Information System*. Intergovernmental Oceanographic Commission of UNESCO.

Oliver, E. C. J., Donat, M. G., Burrows, M. T., Moore, P. J., Smale, D. A., Alexander, L. V., Benthuysen, J. A., Feng, M., Sen Gupta, A., Hobday, A. J., Holbrook, N. J., Perkins-Kirkpatrick, S. E., Scannell, H. A., Straub, S. C., & Wernberg, T. (2018). Longer and more frequent marine heatwaves over the past century. *Nature Communications*, *9*(1), 1324. https://doi.org/10.1038/s41467-018-03732-9

Parmesan, C., & Yohe, G. (2003). A globally coherent fingerprint of climate change impacts across natural systems. *Nature*, *421*(6918), 37–42. https://doi.org/10.1038/nature01286

Pecl, G. T., Araújo, M. B., Bell, J. D., Blanchard, J., Bonebrake, T. C., Chen, I.-C., Clark, T. D., Colwell, R. K., Danielsen, F., Evengård, B., Falconi, L., Ferrier, S., Frusher, S., Garcia, R. A., Griffis, R. B., Hobday, A. J., Janion-Scheepers, C., Jarzyna, M. A., Jennings, S., … Williams, S. E. (2017). Biodiversity redistribution under climate change: Impacts on ecosystems and human well-being. *Science*, *355*(6332), eaai9214. https://doi.org/10.1126/science.aai9214

Perkins-Kirkpatrick, S. E., & Lewis, S. C. (2020). Increasing trends in regional heatwaves. *Nature Communications*, *11*(1), 3357. https://doi.org/10.1038/s41467-020-16970-7

Pershing, A. J., Alexander, M. A., Hernandez, C. M., Kerr, L. A., Le Bris, A., Mills, K. E., Nye, J. A., Record, N. R., Scannell, H. A., Scott, J. D., Sherwood, G. D., & Thomas, A. C. (2015). Slow adaptation in the face of rapid warming leads to collapse of the Gulf of Maine cod fishery. *Science*, *350*(6262), 809–812. https://doi.org/10.1126/science.aac9819

Petraitis, P. S., & Dudgeon, S. R. (2020). Declines over the last two decades of five intertidal invertebrate species in the western North Atlantic. *Communications Biology*, *3*(1), 591. https://doi.org/10.1038/s42003-020-01326-0

Ramalho, Q., Vale, M. M., Manes, S., Diniz, P., Malecha, A., & Prevedello, J. A. (2023). Evidence of stronger range shift response to ongoing climate change by ectotherms and high-latitude species. *Biological Conservation*, *279*, 109911. https://doi.org/10.1016/j.biocon.2023.109911

Richard, B., Dupouey, J., Corcket, E., Alard, D., Archaux, F., Aubert, M., Boulanger, V., Gillet, F., Langlois, E., Macé, S., Montpied, P., Beaufils, T., Begeot, C., Behr, P., Boissier, J., Camaret, S., Chevalier, R., Decocq, G., Dumas, Y., … Lenoir, J. (2021). The climatic debt is growing in the understorey of temperate forests: Stand characteristics matter. *Global Ecology and Biogeography*, *30*(7), 1474–1487. https://doi.org/10.1111/geb.13312

Rosenblad, K. C., Baer, K. C., & Ackerly, D. D. (2023). Climate change, tree demography, and thermophilization in western US forests. *Proceedings of the National Academy of Sciences*, *120*(18), e2301754120. https://doi.org/10.1073/pnas.2301754120

Rubenstein, M. A., Weiskopf, S. R., Bertrand, R., Carter, S. L., Comte, L., Eaton, M. J., Johnson, C. G., Lenoir, J., Lynch, A. J., Miller, B. W., Morelli, T. L., Rodriguez, M. A., Terando, A., & Thompson, L. M. (2023). Climate change and the global redistribution of biodiversity: Substantial variation in empirical support for expected range shifts. *Environmental Evidence*, *12*(1), 7. https://doi.org/10.1186/s13750-023-00296-0

Sanford, E. (2002). Water temperature, predation, and the neglected role of physiological rate effects in rocky intertidal communities. *Integrative and Comparative Biology*, *42*(4), 881–891. https://doi.org/10.1093/icb/42.4.881

Sato, H., Ishida, K., & Noda, T. (2025). Temporal trends of community and climate changes in the anthropocene: 21-year dynamics of four major functional groups in a rocky intertidal

habitat along the Pacific coast of Japan. *Frontiers in Marine Science*, *11*, 1477142. https://doi.org/10.3389/fmars.2024.1477142

Shoals Marine Laboratory. (2018). *Long-term Rocky Intertidal Monitoring on Appledore Island, Maine, 1982-2017* [Dataset]. Environmental Data Initiative. https://doi.org/10.6073/PASTA/B8F52444F86FBEFE97C5BB40673E02D5

Siwertsson, A., Lindström, U., Aune, M., Berg, E., Skarðhamar, J., Varpe, Ø., & Primicerio, R. (2024). Rapid climate change increases diversity and homogenizes composition of coastal fish at high latitudes. *Global Change Biology*, *30*(5), e17273. https://doi.org/10.1111/gcb.17273

Sorte, C. J. B., Bernatchez, G., Mislan, K. A. S., Pandori, L. L. M., Silbiger, N. J., & Wallingford, P. D. (2019). Thermal tolerance limits as indicators of current and future intertidal zonation patterns in a diverse mussel guild. *Marine Biology*, *166*(1), 6. https://doi.org/10.1007/s00227-018-3452-6

Sorte, C. J. B., Davidson, V. E., Franklin, M. C., Benes, K. M., Doellman, M. M., Etter, R. J., Hannigan, R. E., Lubchenco, J., & Menge, B. A. (2017). Long-term declines in an intertidal foundation species parallel shifts in community composition. *Global Change Biology*, *23*(1), 341–352. https://doi.org/10.1111/gcb.13425

Stuart-Smith, R. D., Edgar, G. J., Barrett, N. S., Kininmonth, S. J., & Bates, A. E. (2015). Thermal biases and vulnerability to warming in the world's marine fauna. *Nature*, *528*(7580), 88–92. https://doi.org/10.1038/nature16144

Sunday, J. M., Bates, A. E., & Dulvy, N. K. (2012). Thermal tolerance and the global redistribution of animals. *Nature Climate Change*, *2*(9), 686–690. https://doi.org/10.1038/nclimate1539

Sunday, J. M., Pecl, G. T., Frusher, S., Hobday, A. J., Hill, N., Holbrook, N. J., Edgar, G. J., Stuart-Smith, R., Barrett, N., Wernberg, T., Watson, R. A., Smale, D. A., Fulton, E. A., Slawinski, D., Feng, M., Radford, B. T., Thompson, P. A., & Bates, A. E. (2015). Species

traits and climate velocity explain geographic range shifts in an ocean-warming hotspot. *Ecology Letters*, *18*(9), 944–953. https://doi.org/10.1111/ele.12474

Telwala, Y., Brook, B. W., Manish, K., & Pandit, M. K. (2013). Climate-Induced Elevational Range Shifts and Increase in Plant Species Richness in a Himalayan Biodiversity Epicentre. *PLoS ONE*, *8*(2), e57103. https://doi.org/10.1371/journal.pone.0057103

Thyrring, J., & Harley, C. D. G. (2024). Marine latitudinal diversity gradients are generally absent in intertidal ecosystems. *Ecology*, *105*(1), e4205. https://doi.org/10.1002/ecy.4205

Vasseur, D. A., DeLong, J. P., Gilbert, B., Greig, H. S., Harley, C. D. G., McCann, K. S., Savage, V., Tunney, T. D., & O'Connor, M. I. (2014). Increased temperature variation poses a greater risk to species than climate warming. *Proceedings of the Royal Society B: Biological Sciences*, *281*(1779), 20132612. https://doi.org/10.1098/rspb.2013.2612

Vergés, A., McCosker, E., Mayer-Pinto, M., Coleman, M. A., Wernberg, T., Ainsworth, T., & Steinberg, P. D. (2019). Tropicalisation of temperate reefs: Implications for ecosystem functions and management actions. *Functional Ecology*, *33*(6), 1000–1013. https://doi.org/10.1111/1365-2435.13310

Vinagre, C., Dias, M., Cereja, R., Abreu-Afonso, F., Flores, A. A. V., & Mendonça, V. (2019). Upper thermal limits and warming safety margins of coastal marine species – Indicator baseline for future reference. *Ecological Indicators*, *102*, 644–649. https://doi.org/10.1016/j.ecolind.2019.03.030

Virgin, S. D. S., Denny, M. W., & Schiel, D. R. (2025). The importance of fine-scale refugia and behavioral thermoregulation in the resilience of intertidal limpet populations. *Ecology*, *106*(7), e70155. https://doi.org/10.1002/ecy.70155

Webb, T. J., Lines, A., & Howarth, L. M. (2020). Occupancy-derived thermal affinities reflect known physiological thermal limits of marine species. *Ecology and Evolution*.

1010 Wethey, D. S. (1983). Intrapopulation Variation in Growth of Sessile Organisms: Natural
1011 Populations of the Intertidal Barnacle *Balanus balanoides*. *Oikos*, *40*(1), 14.
1012 https://doi.org/10.2307/3544195
1013 Zarzyczny, K. M., Rius, M., Williams, S. T., & Fenberg, P. B. (2023). The ecological and
1014 evolutionary consequences of tropicalisation. *Trends in Ecology & Evolution*,
1015 S0169534723002732. https://doi.org/10.1016/j.tree.2023.10.006
1016 Zwerschke, N., Bollen, M., Molis, M., & Scrosati, R. A. (2013). An environmental stress model
1017 correctly predicts unimodal trends in overall species richness and diversity along
1018 intertidal elevation gradients. *Helgoland Marine Research*, *67*(4), 663–674.
1019 https://doi.org/10.1007/s10152-013-0352-5

Supplementary materials

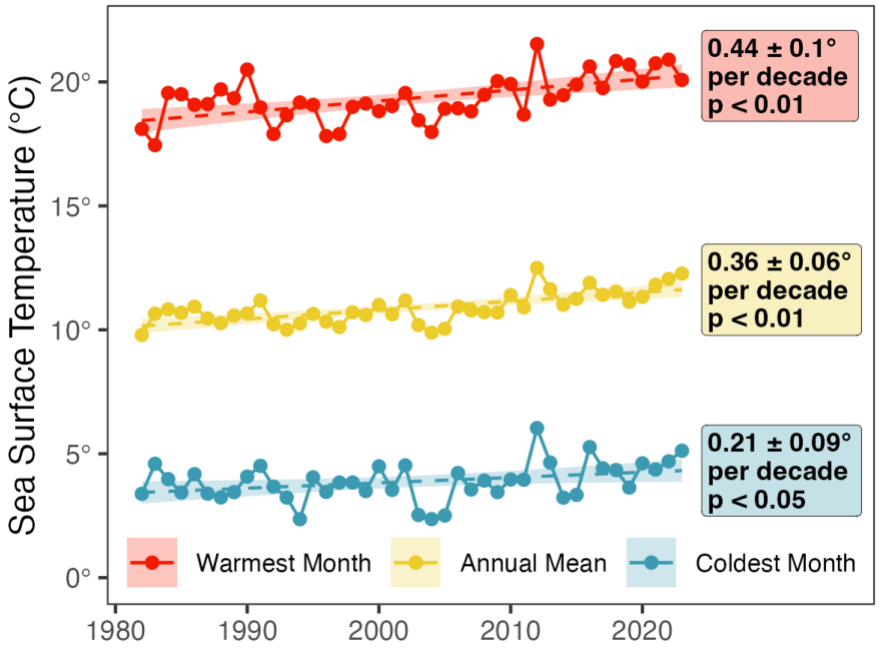

Figure S1. Temperature change on Appledore Island, 1982–2023. Trends of temperature change for coldest month (blue), mean of all monthly temperatures (yellow), and warmest month (red) from the Hadley Centre Sea Ice and Sea Surface Temperature (HadISST) 1° resolution monthly Global Sea Surface Temperature dataset in the cell containing Appledore Island. Points and solid lines show raw values; dotted lines and shaded shadows represent the regression trend ± 95% CI. Model summaries are displayed in text annotations.

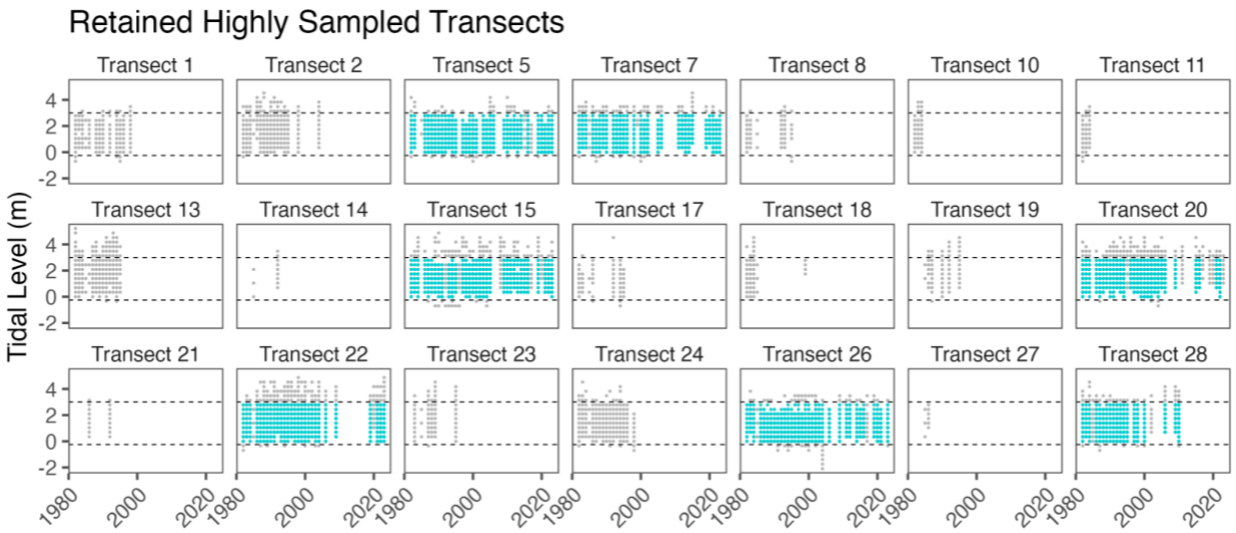

Figure S2. Sampled quadrats retained within the highly-sampled dataset (blue) and sampled quadrats excluded from the highly-sampled dataset (grey). Highly-sampled data were defined as transects sampled for more than 20 years, within nine consistently-sampled shore levels (0–3m, dashed lines). Within these bounds, we excluded transect-years in which six or fewer of the nine remaining levels were sampled, and excluded years in which fewer than three of the remaining nine transects were sampled. In total, the highly-sampled dataset retained 64% of species observations, and 37 of 40 sampled years.

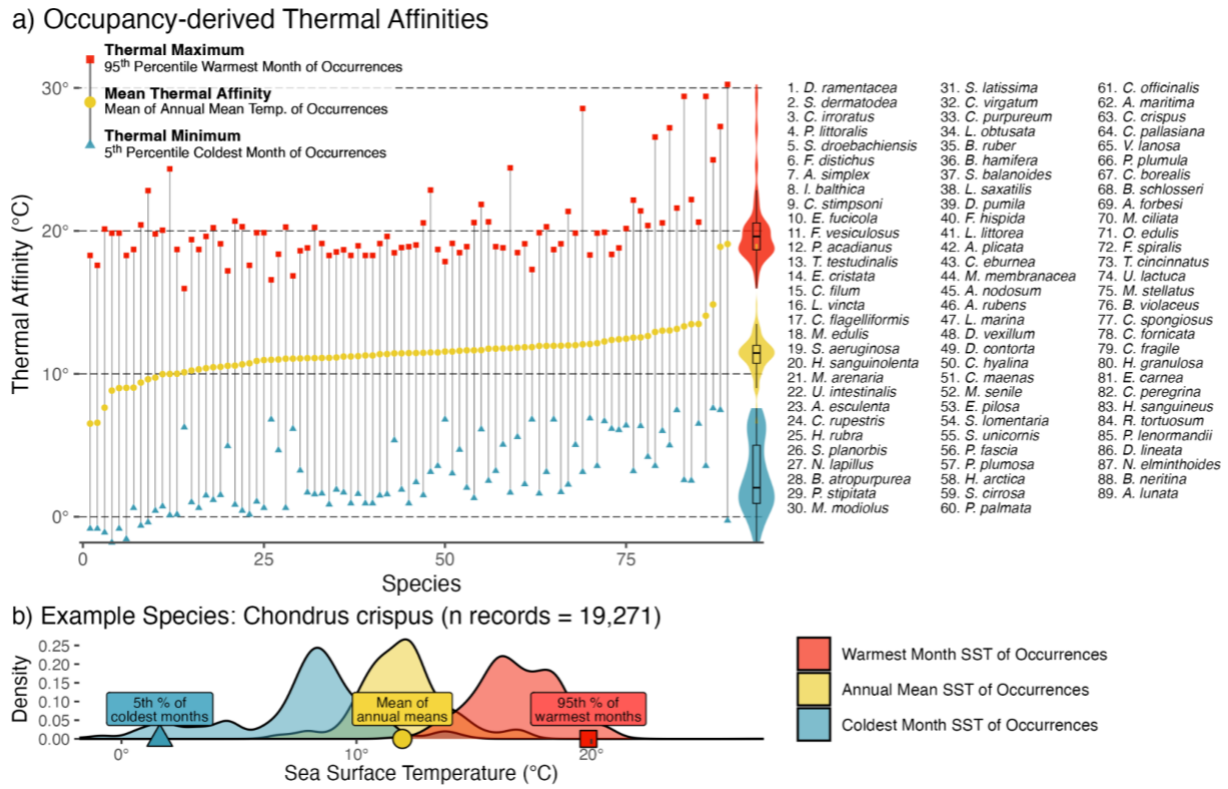

Figure S3. (a) Occupancy-derived thermal affinity values for 89 species on Appledore Island. Each line shows the thermal minimum (5th percentile of the coldest monthly temperature of the year and location of all occurrences; blue triangles), mean thermal affinity (mean of annual mean temperatures of occurrences; yellow circles), and thermal maximum (95th percentile of warmest monthly temperature of the year and location of occurrences; red squares) for each species. Violins and boxplots show the distribution of values for all species. (b) Example distributions of the warmest month, annual mean, and coldest month sea surface temperature in the location and year of 19,271 occurrences of *Chondrus crispus*.

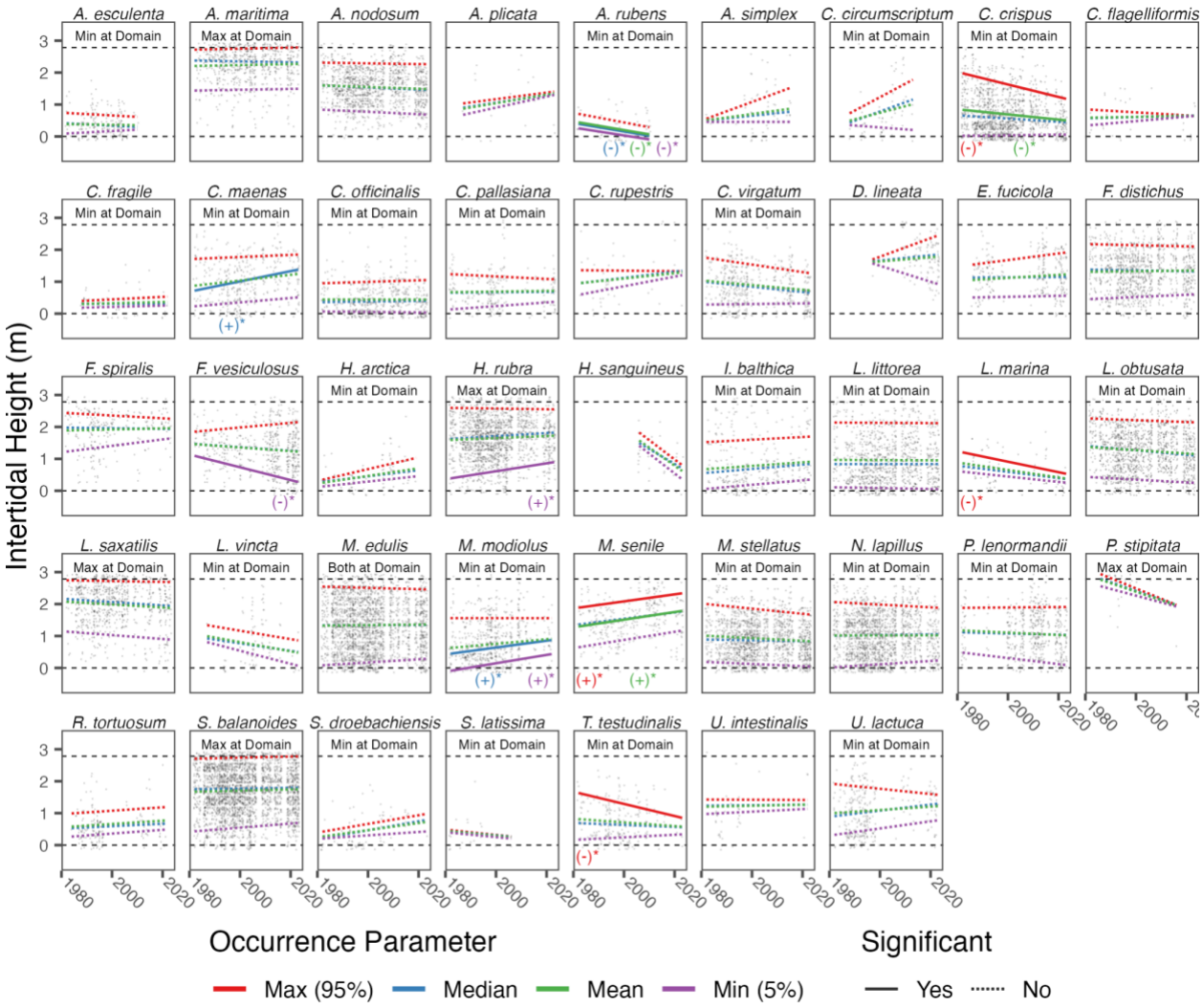

Figure S4. Distributions of all species across intertidal heights over time. Grey dots show species occurrences within nine intertidal heights across seven transects in the highly sampled dataset. Lines show linear regressions of vertical distributional parameters: maximum occurrence height (95th percentile, red), median (blue), mean (green) and minimum (5th percentile, purple), and indicate whether the trend was significant (solid) or not (dotted). Annotations at the bottom of each panel show significant shifts and indicate their direction, (+) for upslope and (-) for downslope. Because shifts outside the sampling domain (dashed horizontal line) might be undetectable, annotations at the top of panels indicate whether a species' range parameter was at the edge of the sampling domain, and was therefore excluded from the edge shift census in Fig. S10.

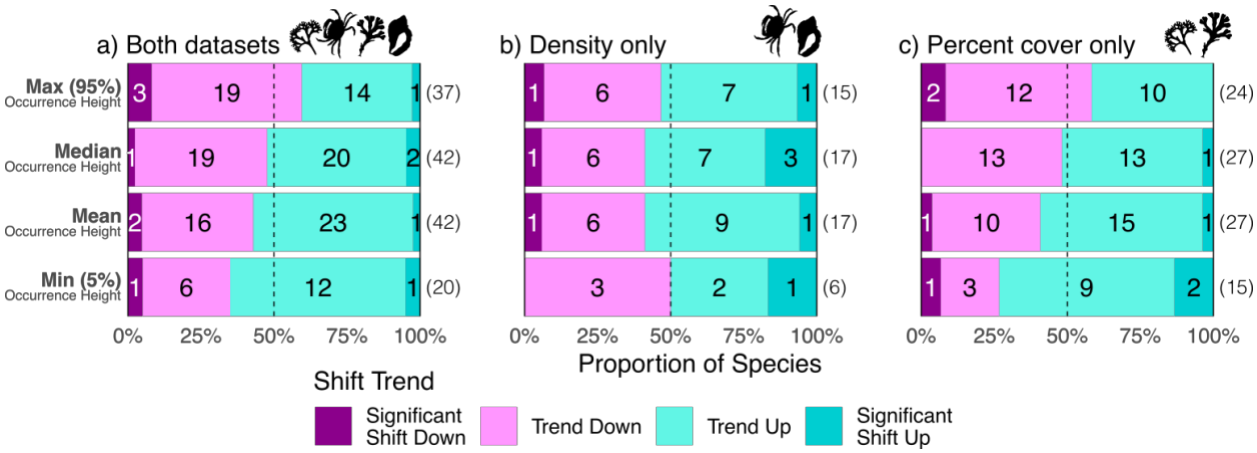

Figure S5. Shifts in individual species' vertical distributions throughout the sampling period, excluding edge shifts when 50% or more of species' annual occurrences were at the highest or lowest sampled height, and excluding mean and median shifts for species that had 50% or more of both their high and low edges at sampling domain edges. Species' metrics are maximum (95th percentile) occurrences, mean, median, and minimum (5th percentile) occurrences in the intertidal zone. Downward shifts are in pink and upward shifts are in turquoise; dark colors show significant trends ($p < 0.05$). Plots show shifts for all species (a), species in the density dataset only (b), and species in the percent cover dataset only (c). Sample sizes are given in parentheses. Note that sample sizes from (b) and (c) may not sum to (a), since some species are present in both datasets and their shifts in (a) are calculated from presences in both datasets combined.

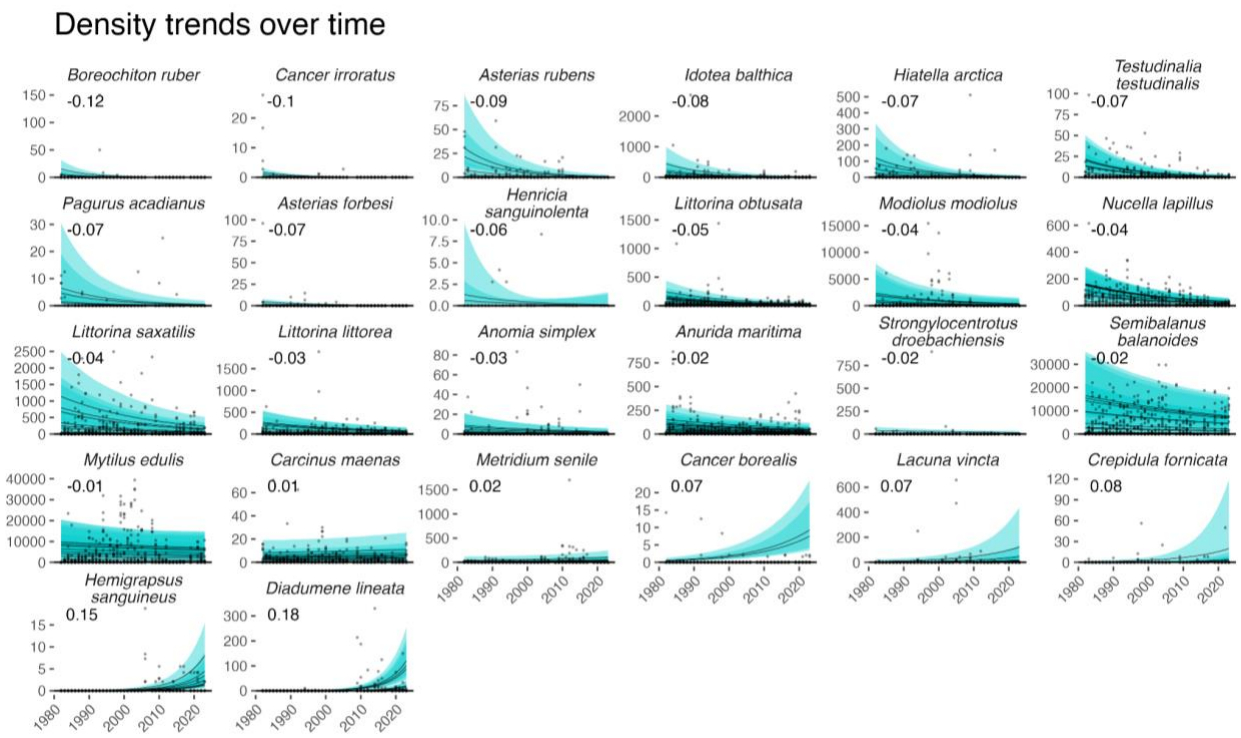

Figure S6. Modeled abundance change trends for all species in the density dataset. Plots show predicted model fits of abundance change using the model formula density ~ year + intertidal height using intertidal height as a fixed categorical variable. Trendlines are shown for each intertidal height, and ribbons show upper and lower prediction intervals within intertidal heights, although the number of intertidal heights represented differs between species. Numbers in the top left show the rounded coefficients of the gamma regression models.

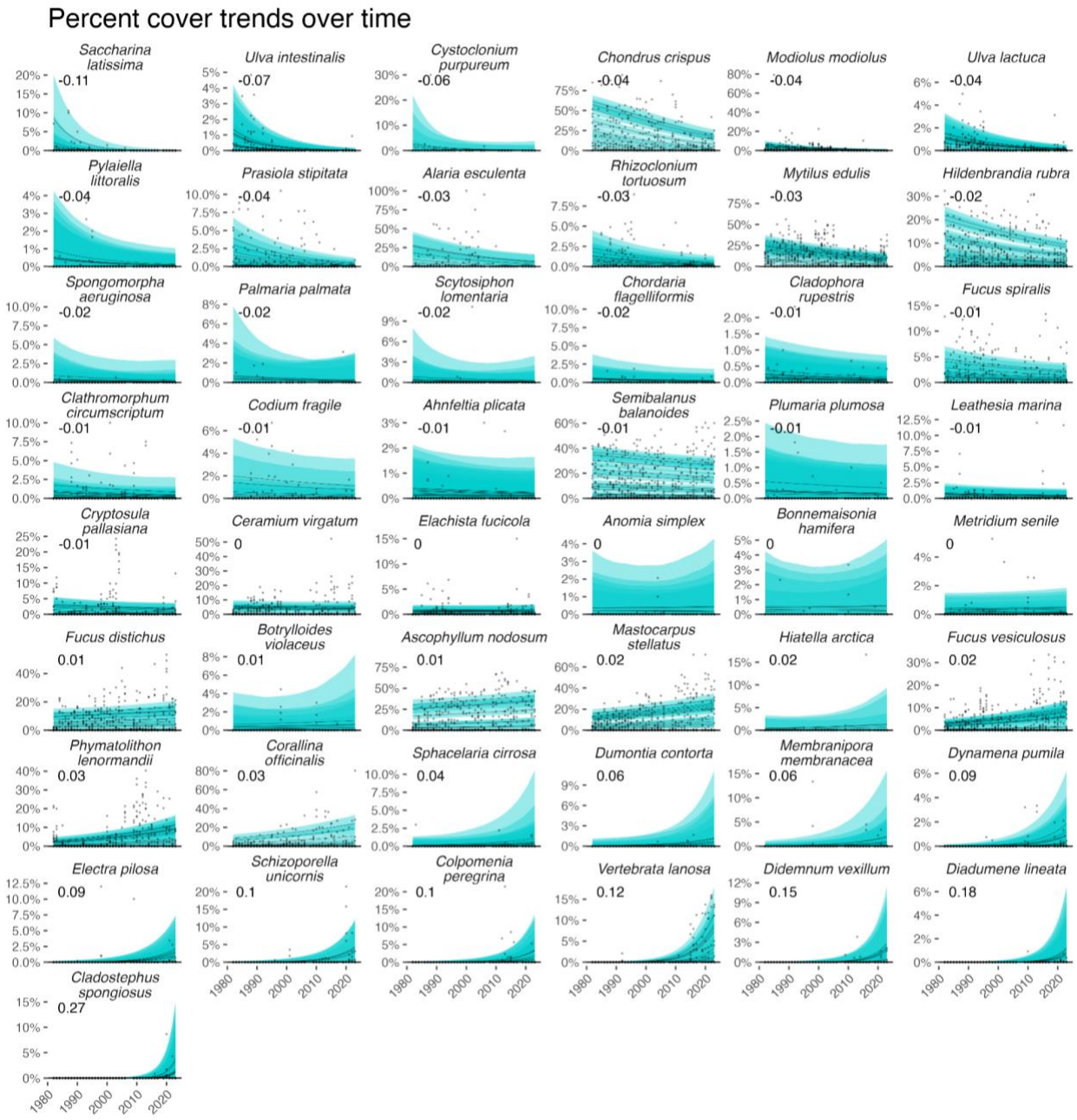

Figure S7. Modeled abundance change trends for all species in the percent cover dataset. Plots show predicted model fits of abundance change using the model formula percent cover~ year + intertidal height using intertidal height as a fixed categorical variable. Trendlines are shown for each intertidal height, and ribbons show upper and lower prediction intervals within intertidal heights, although the number of intertidal heights represented differs between species. Numbers in the top left show the rounded coefficients of the gamma regression models.

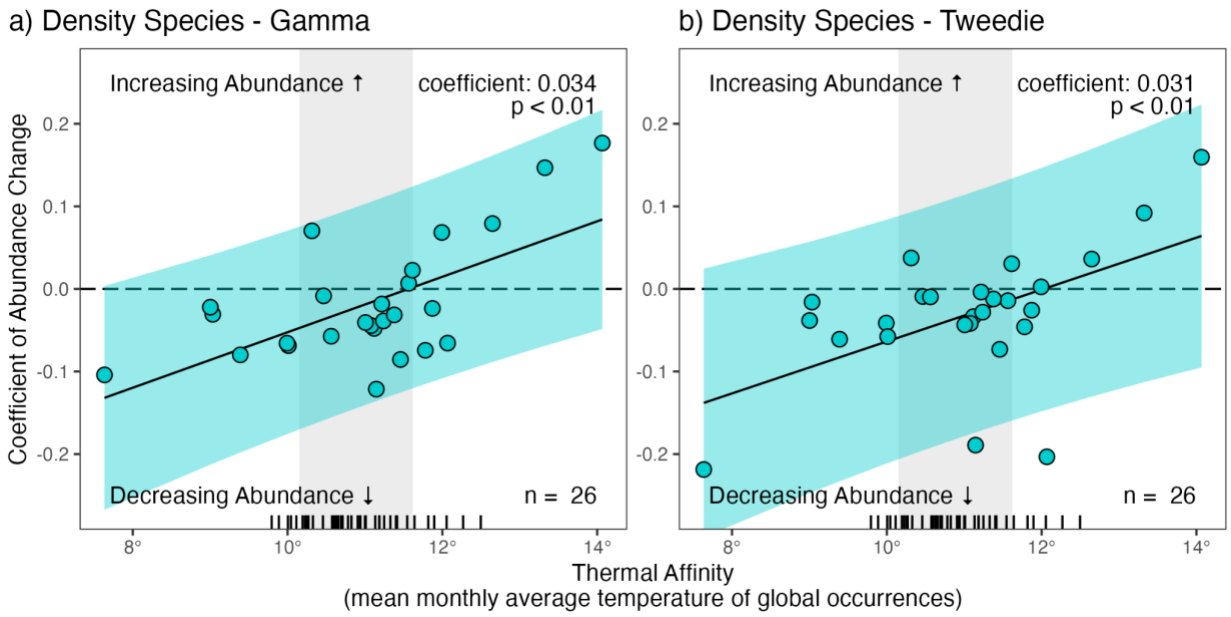

Figure S8. Comparison of thermal affinity to abundance change trends for the density group using gamma (a) and tweedie (b) regression models. Trendlines show the relationship between thermal affinity (average of mean-annual temperatures of global occurrences) and the coefficient of abundance change over time on Appledore Island. Blue shaded areas represent prediction intervals of the regression fits. Vertical grey boxes represent the fitted minimum and maximum values (1982 and 2023) of annual mean sea surface temperature on Appledore Island, and black ticks show the raw values of mean sea surface temperature in all years throughout the study period.

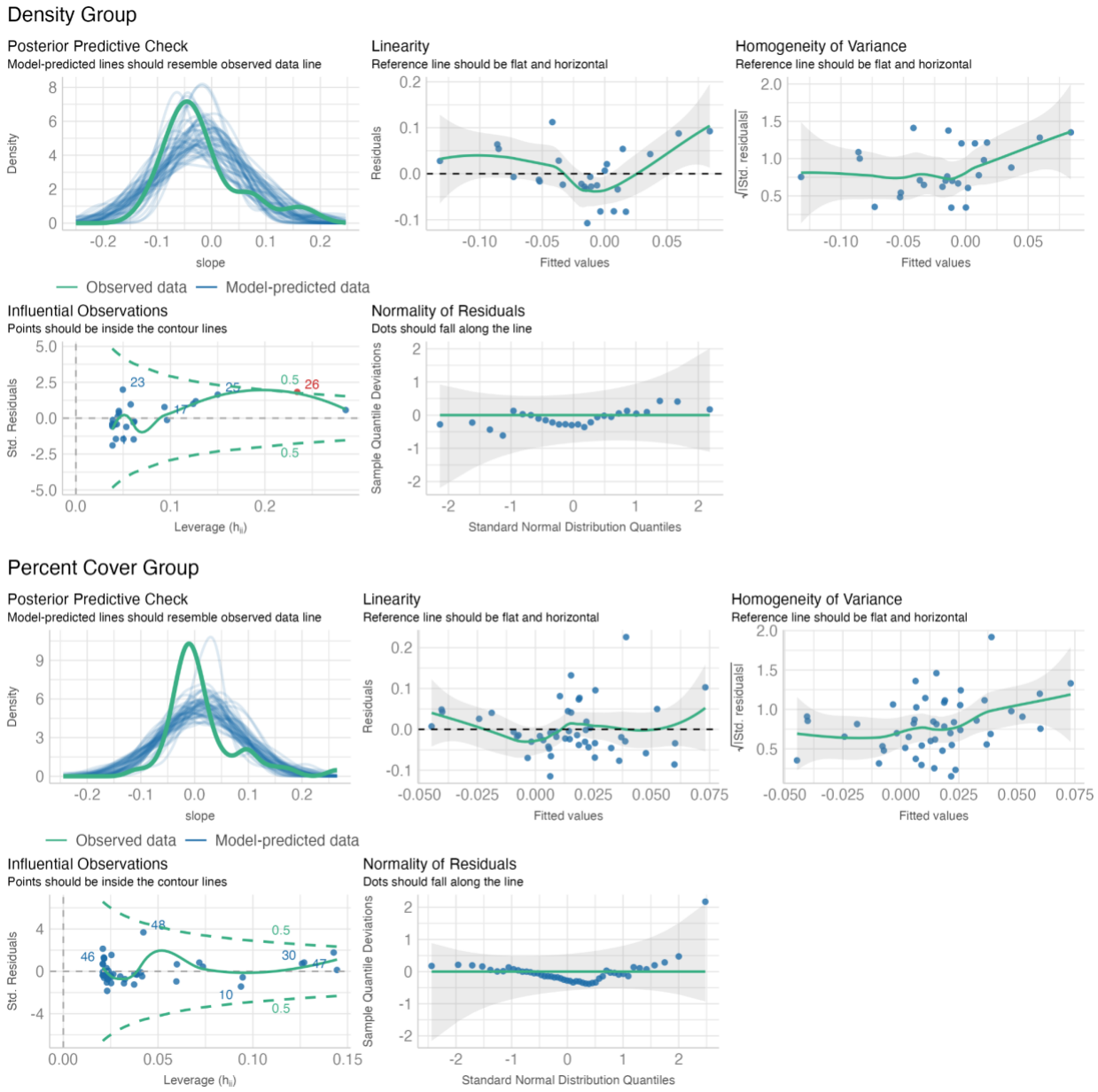

Figure S9. Assumptions check for linear models of abundance change coefficients as a function of species' mean thermal affinities for species recorded as density (top), and as percent cover (bottom).

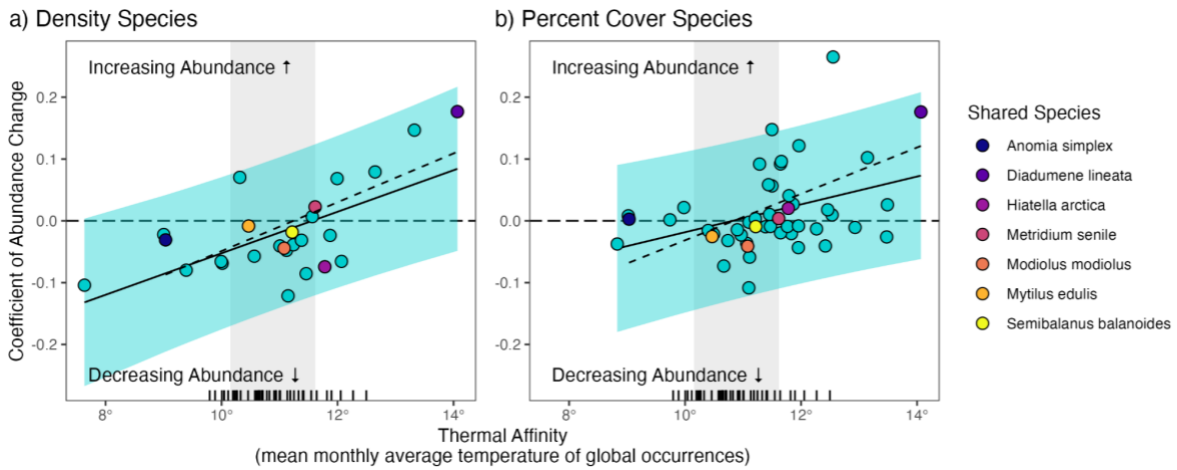

Figure S10. Sensitivity test for abundance change and thermal affinity relationships using only species shared between two datasets, density and percent cover. Background plot is the same as main text Fig. 4, with colored points representing species present in both datasets. Dashed lines show regressions using only the shared species.

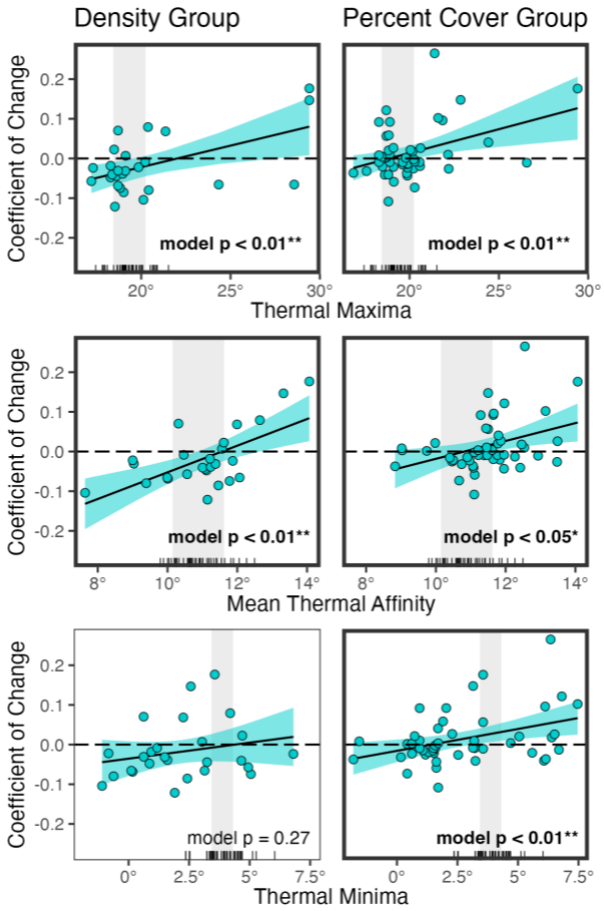

Figure S11, Abundance change coefficients as functions of thermal tolerance. Coefficients of abundance change models for density species (left) and percent cover species (right) as functions of occupancy-derived thermal affinities of minimum (top), mean (middle) and maximum (bottom) monthly temperatures of occurrences. In all plots, black trend lines and blue shadows show the trend and confidence interval of models, points show values for individual species, vertical grey boxes show the range of fitted values of each temperature value throughout the sampling period on Appledore Island, and black ticks show raw temperature values. Thick outlines around plots and text annotations indicate statistically significant models.

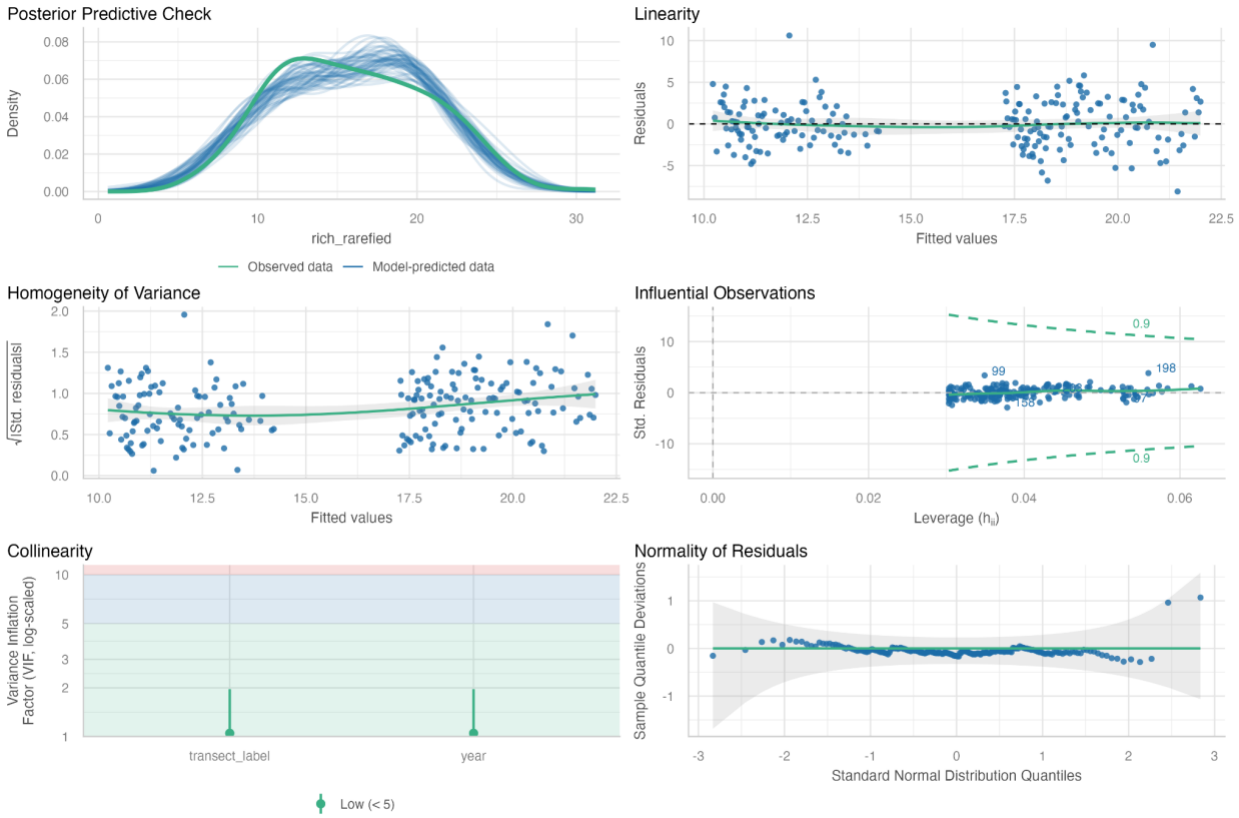

Figure S12. Assumption check for the linear model of total richness over time in seven transects.

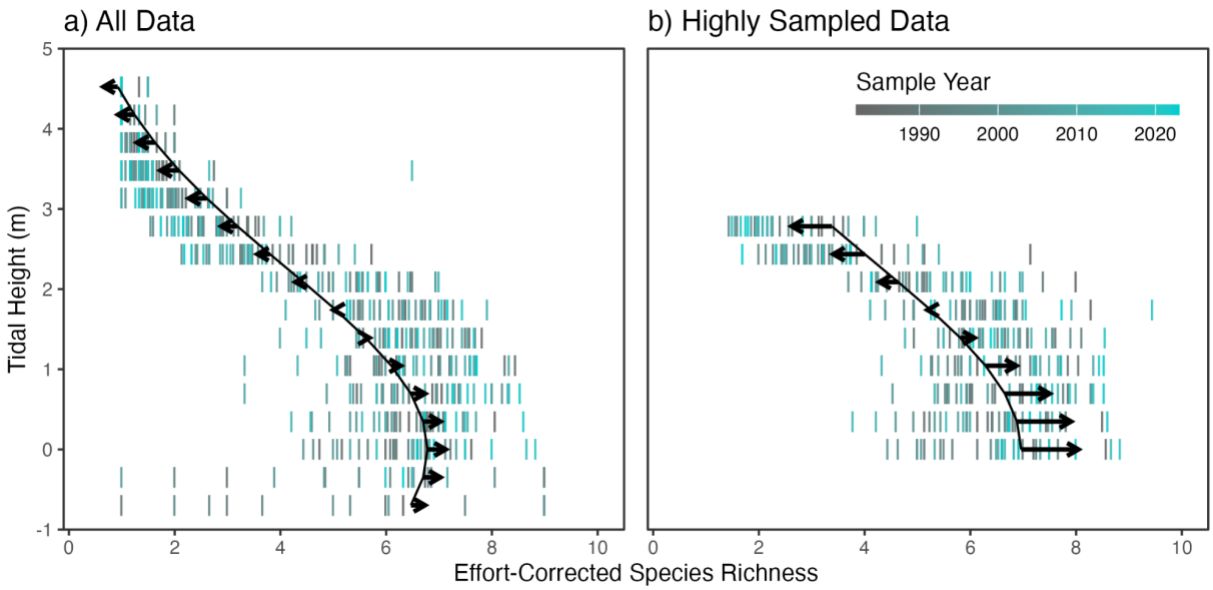

Figure S13. Comparison of richness across depths using all data (a) and highly sampled data (b). In both cases, the best fit model was richness ~ year * intertidal height^2. Colored ticks represent mean species richness across all transects, colored by year. The black curved line represents the model predicted value in the first year of sampling (1982), and arrows show the direction and magnitude of change predicted by the model towards the last year of sampling (2023).

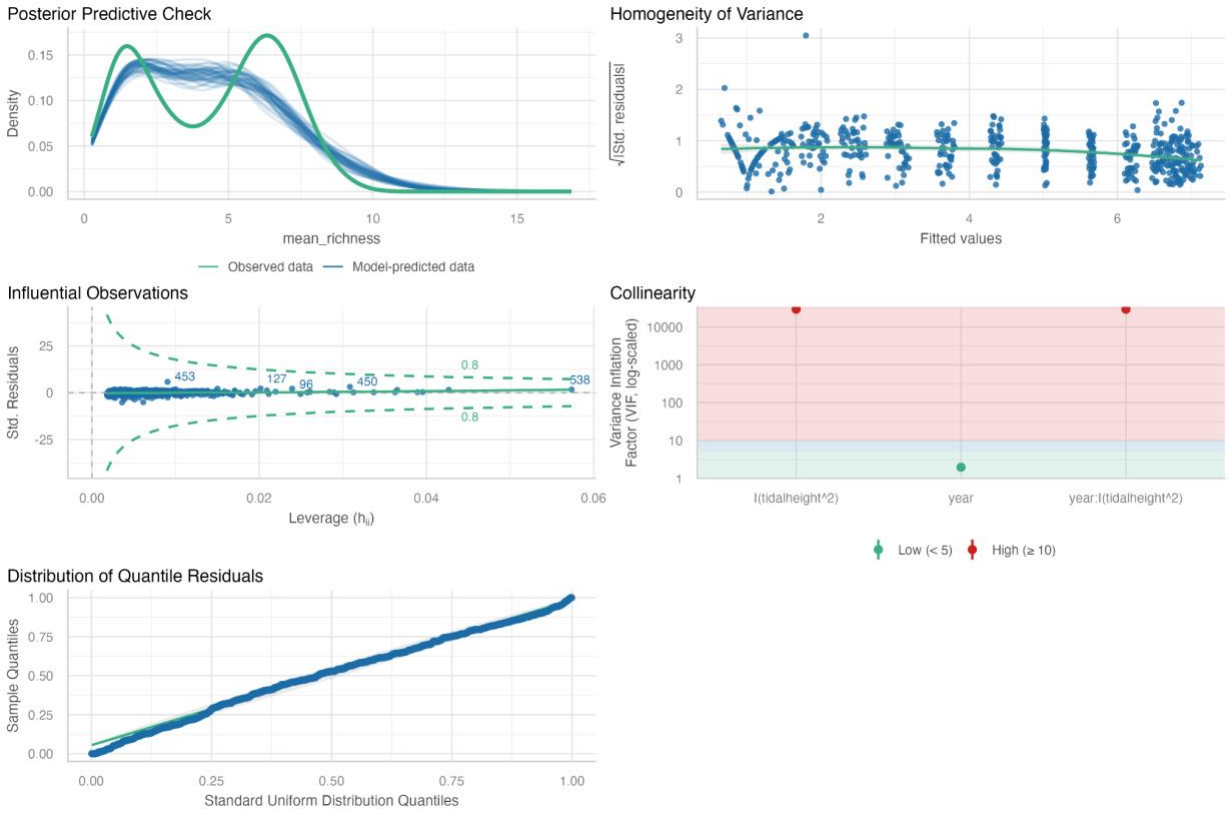

Figure S14. Assumptions check for the generalized linear model of richness over time across intertidal elevations.

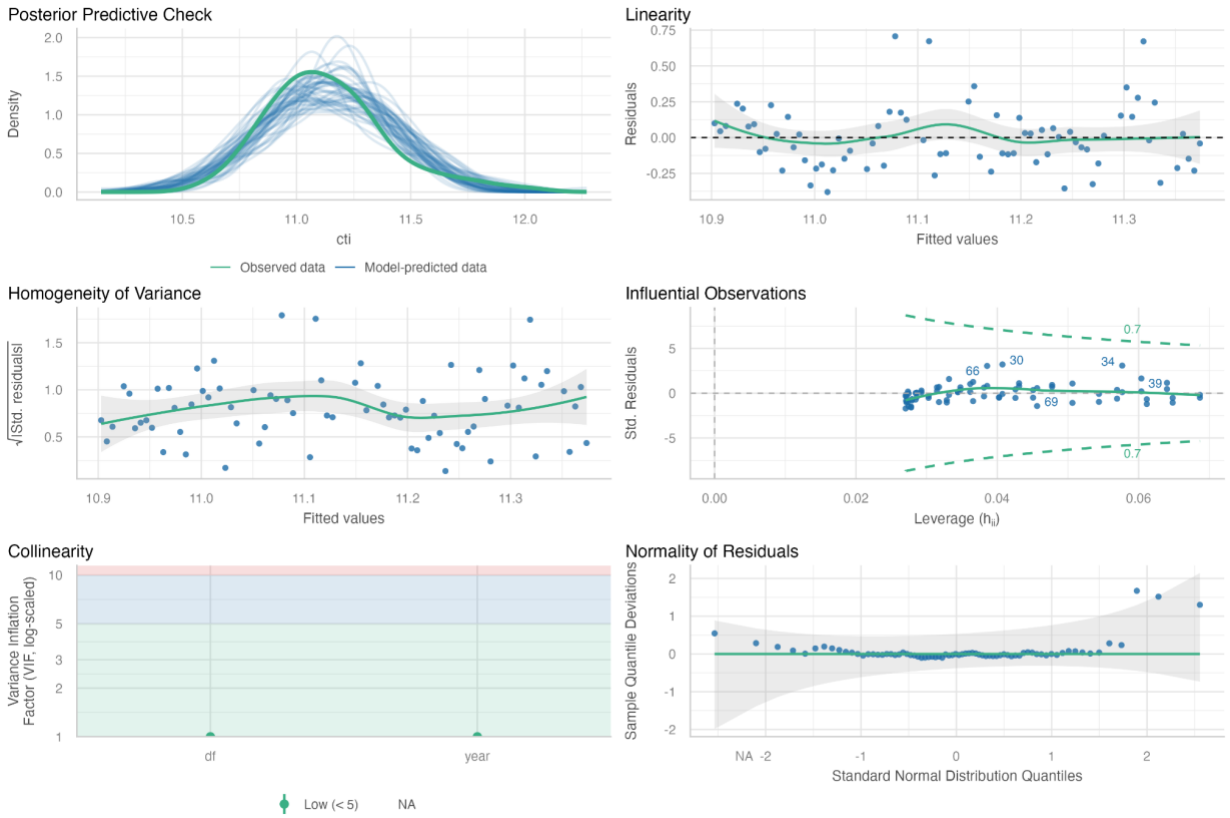

Figure S15. Assumptions check for the linear model of overall community temperature index (CTI) change over time.

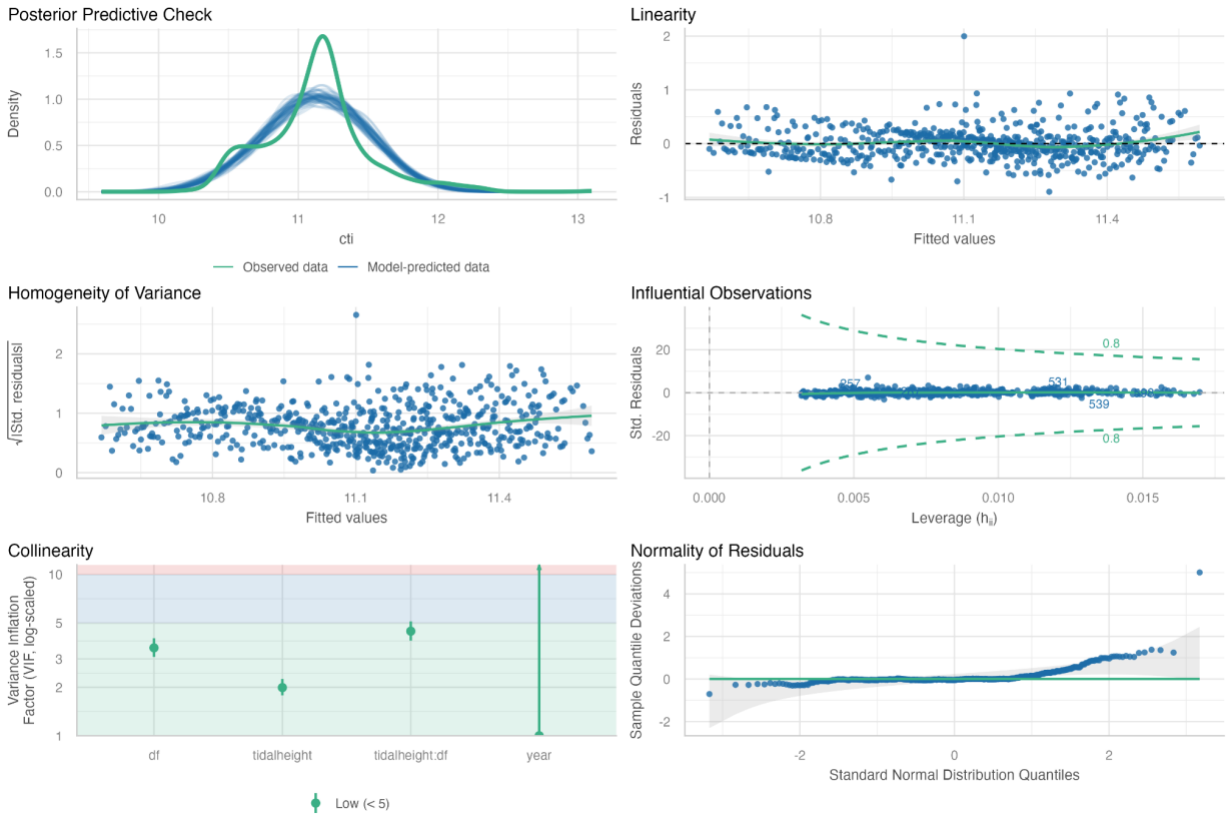

Figure S16. Assumption check for the linear model of community temperature index (CTI) change across intertidal heights and species groups over time.

Table S1. Candidate models for richness across time and intertidal heights. Model formulas and performance values for five models tested to explain richness across intertidal heights across the sampling period. The grey box indicates the best-fitting model, the outputs of which are shown in Fig 5 and Fig S13.

Formula	All Data			Highly Sampled Data Only		
	AIC	AICc	Nagelkerke's R2	AIC	AICc	Nagelkerke's R2
richness ~ year	2533	2533	< 0.01	1385	1385	< 0.01
richness ~ year + intertidal height	1887	1887	0.721	1212	1212	0.425
richness ~ year * intertidal height	1879	1879	0.727	1210	1210	0.433
richness ~ year + (intertidal height)^2	1597	1597	0.838	1108	1108	0.584
richness ~ year * (intertidal height)^2	1591	1591	0.841	1102	1102	0.594

Table S2. Candidate models for community temperature index (CTI) across time and intertidal heights. Grey box shows the model of best fit (lowest AICc value), which was selected.

Formula	AIC	AICc	BIC	R^2
CTI ~ year + intertidal height	518.8	518.8	536.5	0.028
CTI ~ year * intertidal height	520.8	520.9	542.9	0.028
CTI ~ year + intertidal height^2	516.4	516.5	534.2	0.032
CTI ~ year * intertidal height^2	518.4	518.5	540.6	0.032
CTI ~ (year + intertidal height) + species group	394.6	394.7	416.8	0.206
CTI ~ (year * intertidal height) + species group	396.6	396.7	423.2	0.206
CTI ~ (year + intertidal height^2) + species group	391.6	391.7	413.7	0.21
CTI ~ (year * intertidal height^2) + species group	393.5	393.7	420.2	0.21
CTI ~ (year + intertidal height) * species group	209.7	209.8	240.7	0.414
CTI ~ (year * intertidal height) * species group	212.3	212.6	252.2	0.415
CTI ~ (year + intertidal height^2) * species group	253.5	253.7	284.5	0.371
CTI ~ (year * intertidal height^2) * species group	256.7	257	296.6	0.372
CTI ~ year + (intertidal height * species group)	208.2	208.4	234.9	0.413
CTI ~ year + (intertidal height^2 * species group)	251.9	252.0	278.5	0.370
CTI ~ (year * species group) + intertidal height	395.9	396.1	422.5	0.207
CTI ~ (year * species group) + intertidal height^2	392.9	393.1	419.5	0.211

Table S3. Coefficients and p values of linear models predicting species' distributional parameters (maximum occurrence height, median, mean, and minimum occurrence height) as a function of time for all species with sufficient data (n = 43). "Shift" columns show the coefficient for "year" in linear models. Magenta numbers are negative (downslope) and turquoise numbers are positive (upslope). Bold p values are significant (< 0.05). "Domain edge" columns indicate distributions which had over 50% of occurrences at the furthest sampled height, and were therefore excluded in our sensitivity test (Fig S5).

	Max Height (95%)			**Median Height**			**Mean Height**			**Min Height (5%)**		
	Shift (m/dec)	p value	Domain edge	Shift (m/dec)	p value	Domain edge	Shift (m/dec)	p value	Domain edge	Shift (m/dec)	p value	Domain edge
A. esculenta	-0.043	0.683		-0.042	0.543		-0.012	0.851		0.043	0.447	yes
A. maritima	0.017	0.216	yes	-0.015	0.646		0.015	0.654		0.013	0.866	
A. nodosum	-0.012	0.732		-0.034	0.274		-0.028	0.317		-0.037	0.321	
A. plicata	0.103	0.693		0.121	0.66		0.133	0.622		0.173	0.545	
A. rubens	-0.15	0.19		-0.133	**0.038***		-0.135	**0.029***		-0.124	**0.013***	yes
A. simplex	0.291	0.126		0.083	0.406		0.11	0.196		0.001	0.994	
C. circumscriptum	0.421	0.207		0.289	0.286		0.207	0.384		-0.061	0.702	yes
C. crispus	-0.196	**0.000***		-0.05	0.112		-0.081	**0.006***		0.009	0.567	yes
C. flagelliformis	-0.048	0.645		0.019	0.839		0.014	0.879		0.07	0.452	
C. fragile	0.04	0.645		-0.001	0.988		0.019	0.786		0.02	0.79	yes
C. maenas	0.033	0.576		0.161	**0.008***		0.09	0.074		0.068	0.227	yes
C. officinalis	0.024	0.671		0.01	0.767		-0.001	0.985		-0.007	0.657	yes
C. pallasiana	-0.04	0.629		0.007	0.891		0.01	0.828		0.058	0.255	yes
C. rupestris	-0.008	0.961		0.096	0.551		0.082	0.585		0.151	0.318	
C. virgatum	-0.118	0.117		-0.082	0.157		-0.074	0.178		0.009	0.878	yes
D. lineata	0.291	0.143		0.082	0.67		0.065	0.703		-0.249	0.192	
E. fucicola	0.103	0.24		0.006	0.925		0.047	0.339		0.015	0.709	
F. distichus	-0.018	0.723		-0.013	0.744		0.009	0.805		0.035	0.43	
F. spiralis	-0.044	0.389		-0.01	0.881		0.016	0.781		0.101	0.268	
F. vesiculosus	0.073	0.18		-0.056	0.138		-0.057	0.123		-0.2	**0.002***	
H. arctica	0.185	0.125		0.096	0.207		0.12	0.144		0.086	0.25	yes
H. rubra	-0.011	0.652	yes	0.048	0.068		0.033	0.135		0.124	**0.012***	
H. sanguineus	-0.602	0.059		-0.467	0.149		-0.561	0.077		-0.619	0.115	
I. balthica	0.042	0.713		0.068	0.374		0.056	0.393		0.071	0.216	yes
L. littorea	-0.005	0.918		0	0.993		-0.003	0.927		-0.013	0.539	yes
L. marina	-0.164	**0.048 ***		-0.097	0.149		-0.117	0.071		-0.084	0.197	
L. obtusata	-0.029	0.337		-0.07	0.065		-0.052	0.123		-0.044	0.317	yes
L. saxatilis	-0.013	0.485	yes	-0.053	0.291		-0.047	0.248		-0.061	0.429	
L. vincta	-0.132	0.502		-0.117	0.477		-0.144	0.33		-0.206	0.106	yes
M. edulis	-0.021	0.397	yes	0.003	0.919	yes	0.009	0.658	yes	0.049	0.098	yes
M. modiolus	0	0.997		0.107	**0.018***		0.072	0.12		0.131	**0.001***	yes
M. senile	0.11	**0.030***		0.1	0.088		0.12	**0.020***		0.128	0.064	
M. stellatus	-0.08	0.057		-0.013	0.673		-0.042	0.091		-0.034	0.115	yes
N. lapillus	-0.043	0.318		0.01	0.796		0.001	0.982		0.052	0.167	yes
P. lenormandii	0.006	0.93		-0.019	0.795		-0.037	0.556		-0.095	0.141	yes
P. stipitata	-0.322	0.058	yes	-0.274	0.125		-0.268	0.127		-0.211	0.294	
R. tortuosum	0.054	0.585		0.038	0.564		0.051	0.425		0.059	0.415	
S. balanoides	0.017	0.259	yes	0.011	0.63		0.018	0.373		0.064	0.071	
S. droebachiensis	0.135	0.241		0.141	0.159		0.111	0.228		0.054	0.557	yes
S. latissima	-0.083	0.752		-0.07	0.79		-0.076	0.772		-0.077	0.774	yes
T. testudinalis	-0.19	**0.021***		-0.031	0.613		-0.058	0.269		0.04	0.348	yes
U. intestinalis	-0.003	0.987		0.008	0.97		0.016	0.939		0.04	0.865	
U. lactuca	-0.083	0.257		0.096	0.224		0.053	0.42		0.112	0.192	yes